Comparison and Integration of Frequency multiattributes in thin layer visualization: a Stratton field case Study

……..

A Thesis

Presented to

The Faculty of the Department of Earth and Atmospheric Sciences

University of Houston

……

In Partial Fulfillment

Of the Requirements for the Degree

Master of Science

……

By

ATEKPA, MUSA IBRAHIM

May, 2014

Comparison and integration of frequency multiattributes in thin layer visualization: a Stratton field case study

_____

Atekpa, Musa Ibrahim

APPROVED BY:

_____

Dr. John Patrick Castagna, Professor
(Committee Chair)
Department of Earth and Atmospheric Sciences
University of Houston

_____

Dr. Evgeny Chesnokov, Professor
Department of Earth and Atmospheric Sciences
University of Houston

_____

Dr. Donald Kouri, Professor
Department of Physics,
University of Houston

_____

Dean, College of Natural Sciences and Mathematics
University of Houston

Dedication

Verily all praises and thanks are due to Almighty God for granting me the bulldog persistence to hold on against all odds. This work is dedicated to Uncle Jafaru, Muhammad Atekpa (Sardaunan Opanda) for his unrelenting support.

Acknowledgements

Greatness is not measured by the amount of accolades or encomiums conferred on one. In my opinion, it should be accessed based on the combination of intelligence and the action of the limbs to help others actualize their dreams. I want to unreservedly thank my advisor, Professor John Castagna for his help and patience during this research. Thanks a lot for teaching me that a crawling child can one day learn to walk if he tries hard enough.

I would like to profoundly thank other members of my thesis committee, Professor Evgeny Chesnokov and Professor Donald Kouri for their contribution and also for their patience. I want to thank the President of Lumina Geophysical, Carlos Moreno, for granting me access to his company's resources over the entire summer period. I would also like to extend my appreciation to Alejandro Juranovic for providing me with a processed data and Jian Zhou for allowing me access to his code.

I want to extend my deep appreciation to Arnold Oyem, Ayodeji Babalola, Ernest Nwoye (Chief the man), Maria Amirzadeh, Yahaya Abubakar, Muhammad Shogar and host of my other friends. My profound gratitude goes to Kalu Udonsi for being more than a brother to me in a place far away from home. Thank you for always resonating at the same frequency with me. You prevented me from tuning out in different circumstances.

I want to thank members of my family for their understanding. I want to thank my dad for his moral support, my mum for her fervent prayers, and ultimately Uncle

Jafaru Muhammad Atekpa for his unrelenting support. Thank you all. If it is possible for me to pull down the rainbow, I will write your names in gold letters and put it back in the sky to show the whole world how grateful I am for providing that strong shoulder for me to lean on.

Comparison and Integration of frequency multiattributes in thin layer visualization: a Stratton field case study

……..

An Abstract of a Thesis

Presented to

The Faculty of the Department of Earth and Atmospheric Sciences

University of Houston

……

In Partial Fulfillment

of the Requirements for the Degree

Master of Science

……

By

Atekpa, Musa Ibrahim

May, 2014

ABSTRACT

The choice of the right analysis window size in spectral analysis helps to capture the best thickness variability associated with tuning effects in thin layers. This research is a fidelity comparison to resolve thin stratigraphic features in the Stratton field, between spectral decomposition methods such as Discrete Fourier Transform (DFT), Continuous Wavelet Transform (CWT) and Constrained Least Squares Spectral Analysis (CLSSA), which is an inversion-based algorithm that computes spectral decomposition. Resolution of a 'D' sand series channel in-fill sandstone with splay deposits of the middle Frio Formation is superior using the inversion method at different analysis windows. Integration of the attributes is done in a synergistic manner to go beyond the limit of spectral decomposition using multivariate analysis to visualize subtle features. At smaller spectral decomposition analysis window and larger Principal Component analysis (PCA) windows respectively, results shows that the Fourier method, though having a fluctuating Heisenberg Uncertainty product at peak spectral frequencies, produces an enhancement beyond the spectral decomposition bandwidth limit due to stronger correlation of the attribute frequencies after axis rotation in its principal components. Finally, the multiplicity observed in the energetic trends of the frequency spectra is combined to enhance the stratigraphic features using primary colors.

TABLE OF CONTENTS

LIST OF FIGURES

FIGURES (APPENDIX)

CHAPTER ONE

INTRODUCTION

1.1 General Introduction

The goal of most seismic interpretation is to extract qualitative or quantitative information from each basin as much as possible. This is achievable by searching through the data looking for anomalous seismic response even in minute details. Interference patterns and tuning effects from thin beds hinder these objectives.

The seismic data contain dispersive information resulting from the band limited nature of the source wavelet. Subsurface reflectors filters the long wavelength (low frequency) allowing the information to spread over a large part as it propagates. Due to the size of the wavelet, beds smaller than the width of the wavelet are impossible to be resolved on the seismic. Bed thickness and acoustic contrasts are significant properties that makes them visible seismically. Hence, thick beds with low acoustic contrasts may be invisible depending on the amount of signal- to- noise ratio in the data. Conversely, thin beds may be visible seismically depending on the acoustic contrasts of the embedding medium (Brown, 2011).

Constructive interference occurs at tuning thickness between the top and bottom of thin layers. That point where the bed thickness reflection from the top and bottom are inseparable is known as tuning thickness. Two phenomena that explain the concept of tuning in thin layers are amplitude and frequency tuning. Amplitude tuning occurs at maximum amplitude for a bed thickness at $1/4^{th}$ the dominant wavelength, or

½ period of the dominant energy. For beds thinner than this, thickness depends on the shape of the composite wavelet and the frequency content. At this point, the shape of the wavelet remains the same but the amplitude decreases and higher frequencies are required to image thinner beds. Frequency tuning on the other hand occurs for layer thicknesses at $1/4^{th}$ period of the dominant energy or less (Brown, 2011). However, beyond $1/4^{th}$ of the dominant wavelength, that is at $1/8^{th}$ the dominant wavelength, destructive interference takes place. Resolution and detection of a bed is achieved in this scenario by removing the effect of the source wavelet.

Spectral decomposition reveals spatially the reservoir heterogeneity occurring within the bandwidth of a seismic signal in response to interference patterns. This method provides greater resolution of thickness variation and spatial extent of geologic features using their tuning frequencies as the beds tune in and out. Different spectral decomposition techniques have been used over time in an attempt to improve the vertical resolution of the seismic. Fourier methods such as Fast Fourier Transform (FFT), Discrete Fourier Transform (DFT) were the first to be used. Improvements in extracting more qualitative resolution saw the introduction of the wavelet transforms such as the Discrete Continuous Transform (DCT), Continuous Wavelet Transform (CWT). Other methods are being introduced to the industry including an inversion-based algorithm that is an improvement on the Fourier transform that can compute spectral decomposition, which is Constrained Least Squares Spectral Analysis (CLSSA). Partyka et al., 1999 used the Fourier transforms with a short window to determine thickness of

thin layers, Castagna et al., 2003 used the Wavelet Transforms in Instantaneous Spectral Analysis to detect gas shadows in reservoirs.

A significant characteristic of an attribute is that they are unique and must not be independent from each other. Similarity in the output volumes from spectral decomposition creates a lot of data redundancy. Multiattributes analysis techniques were introduced to reduce the overwhelming information from different attributes to only the most significant representing the feature of interest. Principal Component Analysis (PCA)is a nonlinear multiattribute technique that rotates the axes of the data coordinates unto a new dimension such that the new coordinates are representative of the original data but provide higher degree of variance. Spectral attributes volumes each highlight an aspect of a feature on a horizon that is ''in-tune'' with that frequency, which may be on the high or low end of the frequency spectrum. Rotating the coordinates will preserve all the smaller aspects as the image is in the subsurface without interference effect. Principal Component analysis even though a statistical tool that was first used by Pearson (1901) and Hotelling (1933), it has been utilized in geophysical pattern recognition studies. Guo et al., 2008, used Match Pursuit decomposition to interpret features on the Atoka Unconformity. Puryear et al., 2008 compare the results from PCA using continuous wavelet transform and Match Pursuit decomposition, to sharpen lateral resolution of stratigraphic features in a complex turbidite model.

Thin geological features are better resolved with a running window. Using the entire length of the seismic trace will be defective in recognizing thickness variability

associated with tuning effects in thin layers. Windowing the data has the potential to mask or enhance the spectra of the data depending on the spectral decomposition method in use. In this thesis, I will use different analysis windows to get the best variability in resolution that best describes the stratigraphy within my area of interest. Generally increasing the window size in spectral decomposition forfeits the temporal resolution as the spectral resolution is enhanced. However, wavelets with long taper windows decrease the spectral resolution.

1.2 Motivation/Statement of the Problem

The Stratton field, especially the Middle Frio formation has a lot of thin beds as stratigraphic traps which may be as thin as 5 feet in some areas. Resolutions of the reservoir units fall below seismic resolution therefore bypassing some of the prospects during exploration. Layer interference patterns obscure subtle stratigraphic features that are probable prospects. The absence of a P-wave sonic log in the suite of well logs adds in part to the problem encountered to characterize this field. Generation of a pseudo velocity log using a popular rock physics transform to make up for the absence of sonic log in the suite of logs in the data set, creates lot of uncertainties because the transit time of the seismic wave is simulated from a nearby log. Signature of the reservoir zones on the well logs during well tie may not be accurate as they are only derivative of another log response to the physical characteristics of the earth. The use of frequency multiattributes in the midst of these challenges will help us to characterize this field better.

1.3 Objectives

Reviewing geophysical publications reveals that there are different spectral decomposition algorithms are out there each having its pros and cons depending on your needs at the instant. In this work, I will compare and integrate three popular algorithms to determine which has a better capability to visualize subtle features in this prolific basin. Integration of the algorithm with the best fidelity into principal component analysis will be carried out with the objective to go beyond the bandwidth limit of spectral decomposition to view subtleties. Having stated that, would it be possible to go beyond the practical limit of spectral decomposition attributes to visualize subtle features? That remains for us to find out as we go on. This is the basis for this research.

1.4 Research Scope

This thesis will compare different spectral decomposition attributes to identify which of them has a better resolution potential to visualize the subtle stratigraphy of the Middle Frio formation. Spectral decomposition dissociates the frequency bandwidth of the seismic data into individual frequencies, such that each frequency is a representation of the subsurface architecture. This technique helps interpreters to unravel features below seismic resolution.

In this research work, chapter one is dedicated to the introduction. Chapter two is on the theoretical background of the algorithms used in this work. I started off with the Fourier Transform and discussed about the Discrete Fourier Transform which is the

most popular type of Fourier Transform readily used in the field of Geophysics. Next I talked about the Wavelet transform by focusing on the continuous wavelet transform. Lastly I talked about inversion and spectral inversion briefly. I went on further to discuss about CLSSA, the algorithm that can compute spectral inversion as well spectral decomposition. Finally in that chapter, I wrote about the geology of the Stratton Field and analyzed a well tie that forms the basis for this research work. In Chapter Three I made a comparison between the frequency maps of the three algorithms analyzing their resolving potentials on the stratigraphic features on a horizon. Chapter Four is on the theory and applications of Principal component analysis. Later on in that chapter, I wrote about spectral color blending. Chapter Five is on summary and conclusions. This is the scope of this work in a concise manner.

CHAPTER TWO

THEORY OF SPECTRAL DECOMPOSITION AND GEOLOGY OF THE STRATTON FIELD

2.1 Introduction

Vibrations of energy propagating through the earth are recorded to understand the varying characteristics of the subsurface geology. The signals acquired in time are combinations of subsurface reflections, backscattered surface waves and interference patterns. A seismic trace is a single wave field recorded in time at a particular receiver location. Transforming the seismic trace from the time domain to another domain aids an interpreter to unravel subtleties, making this tool to be unparalleled in qualitative seismic pattern recognition. In this chapter I will take a look at the theory defining the most popular spectral decomposition transforms. In addition, the geology of the Stratton field and well calibration information will be emphasized in this section.

Understanding the complex seismic trace over the past couple of decades has translated into a huge number of generated seismic attributes. Attributes are quantities that are derivatives from the seismic data to give us information about the nature, structure and fluid characteristics in the different lithological layers. Over time authors have classified attributes in different ways. Brown (2011), classified attributes into four major classes that are each subdivided into pre-stack and post-stack attributes. The main classes are: Time, amplitude, attenuation and frequency. The first three has been studied extensively to provide information about structure, fluid saturation and

permeability. Frequency has not been fully studied but there are speculations that it can provide us with information about fluid saturation and nature of stratigraphy.

The non-stationary nature of seismic signals makes it possible to create a varying time-frequency signatures of the subsurface geology. Transforming the signal from time to frequency reveals subsurface details that are obscured by interference patterns in the frequency spectrum. Spectral decomposition is computed using mathematical methods such as Fourier transforms and Wavelet transforms to change a signal from the time domain to its frequency equivalence. Inception of this method revolutionized the world of seismic interpretation by providing high fidelity spectral maps of amplitude and phase components, in delineation of stratigraphy and structural orientation. This technique has been exploited to reduce uncertainties in drilling of dry holes, and facilitates the integration of geology and seismic in reservoir simulation.

Partyka et al., in 1999 introduced this concept and demonstrated how a windowed Discrete Fourier Transform (DFT) can be administered in thin bed thickness estimation. Peyton et al., 1998, used spectral decomposition along with coherency to interpret incised valley stratigraphy. Castagna et al., 2003, used Match Pursuit Decomposition (MPD) for Instantaneous Spectral Analysis (ISA) to detect low frequency shadows beneath reservoirs.

Spectral decomposition creates amplitude and phase from each frequency value to detect the tuning frequency that highlights the best thickness from a tuned seismic response. In explaining the concept of spectral decomposition, Partyka et al., 1999, built on the Widess (1973) concept of thin layer reflectivity model of reflections

from a porous layer that is sandwiched between hard matrix materials. Variation in the spectral content is due to acoustic properties of the thin layers to interference and bed thickness. They based their concept on the illustration as shown in figure 1. Assuming that the magnitudes of the reflections from the thin layer are equal and opposite, a composite reflection will appear as a tuned response on the seismic. When Fourier transformed, a series of spectral notches seen as sharp edges in the frequency spectrum will be observed. Reciprocal of a frequency notch value gives the bed thickness of the thin layer which is significant in reservoir volumetric.

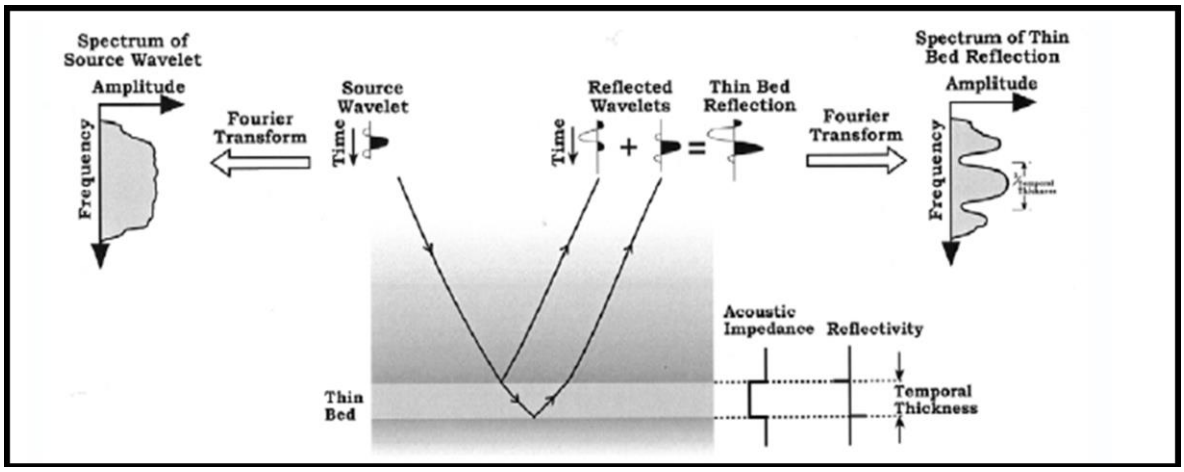

Figure 1 Illustration of Thin layer reflectivity in layer thickness estimation (Partyka et al., 1999)

2.2 Spectral Decomposition Methods

Different spectral decomposition methods have been developed with particular objectives in mind. The most popular are the Fourier Transforms and the Wavelet Transforms. Another method that will be an integral part of this thesis is the Constrained Least Squares Spectral Analysis (CLSSA), which is an inversion algorithm that can compute spectral decomposition, a modification upon the Fourier Transforms. This subsection shall be about dissecting the different transforms.

2.2.1 Fourier Transform

In the field of Science and Engineering, vibrations or waves of energy are studied by the nature of the signal and shape of its associated spectrum. The waveform of these signals contains multiple frequencies with variations in amplitude and phase depending on the signal strength. Signal of this nature embodies a series of functions that are sinusoidal variations in time but also representative in the frequency domain.

Fourier transform is a mathematical concept that transforms a signal or continuous time series from the time domain into the frequency domain. This transformation is advantageous due to the flexibility of the operation to be looped back and forth in the frequency domain, an action that facilitates noise suppression, which is inconceivable in the time domain. Fourier transforms deals with summations of symmetric functions at different frequencies. If we have a continuous function variable t, the forward Fourier transform of t is:

$$\mathbf{F(w)=} \int_{-\infty}^{\infty} \boldsymbol{f(t)e^{iwt}dt} \text{.....i}$$

Where e^{iwt} is the kernel function, angular frequency w, is related to the linear frequency by w=2πf, g(t) is the time function and g(w) is the complex function that can be expressed in the polar form as g(w)=A$e^{i\theta}$. A (w) gives the amplitude spectrum and θ (w) the phase spectrum. Information about time is absent in the amplitude spectrum but encoded in the phase spectrum. This makes time localization in Fourier transform a challenge.

Fourier analysis gives a summation of sines and cosines to give a weighed sum known as sinusoidal basis functions. In seismic data applications or analysis, cross correlation of the sinusoidal basis functions with the seismic data gives a spectral function. A condition that must be met when dealing with basis functions is that they must be orthogonal. Extraction of amplitudes from a signal in time is accomplished with the orthogonality property of the Fourier transforms which states that 'if you take a sine and cosine, or two cosines, each a multiple frequency of the fundamental frequency, multiply them together and integrate the product over one period of the frequency, the result is always zero, except in special cases.

Fourier transform is a fundamental tool used in mathematical topics such as linear algebra for vector representation as orthonormal basis or in linear combination of eigenvector matrix. Historically, the theory was formulated by a French mathematician and Physicist Jean Baptist Joseph Fourier (1768-1830), in one of his popular works that was initially rejected. He postulated that the heat distribution can be represented by a series of sinusoids, and a continuous signal is a summation of sinusoidal waveforms. Lagrange and Laplace were the foremost scientists alive at that time but they took different sides to the credibility of his claim. Laplace agreed with Fourier on his theorem, but Lagrange objects to it as he said the hypothesis will not hold for discontinuous signals such as square waves. It was after the death of Lagrange that the theory saw the light of the day. It was discovered later that the theory holds for summation of sinusoids where the difference is near zero. This scenario later became to be known as the Gibb's phenomenon.

Properties of the Fourier Transform

Similar to other mathematical techniques, the Fourier transform has properties that make it suitable for applications in many fields. The Fourier transform has the characteristics of linearity and convolution which makes it one of the most useful properties. Convolution is a mathematical operation that multiplies one time series against another. A signal that is convolved in time domain corresponds to multiplication in the frequency domain and vice versa. Application of this concept is ingrained in discrete Fourier transform, filter analysis etc. Shifting is another property that is observable either in the time or frequency domain by utilizing the phase component of the signal.

2.2.1.1 Discrete Fourier Transform

Discrete Fourier Transform is a mathematical technique that transforms a signal or data sampled as periodic summation at discrete intervals, into series of complex sinusoids having ordered frequencies. When a real sequence of number is discretely transformed, the output will be a sequence of numbers having similar length. The output frequencies are usually multiple integer of fundamental frequency. DFT has found applications across various disciplines. It is used in image compression; signal processing, partial differential equations etc.

In non-stationary signal applications such as seismic signal analysis, DFT performs a cross correlation between the seismic trace and the sinusoidal time series within a moving window. Transformation from the time to frequency makes it multidimensional, as there is a truncation of the time series within the small analysis

window leading to amplitude smearing. This windowing problem is one basic limitation of DFT. Utilization of this transformation in geological interpretation of anomalies or structure gives poor spectral resolution at small intervals and high spectral resolution at high time intervals respectively. A concept of windowing in Fourier analysis called Short Time Fourier Transform (STFT) was introduced by Gabor (1946) to analyze a portion within a signal instead of the entire signal. The portion within a segment of the signal is assumed to be stationary, or rather treated as stationary signals. In seismic analysis, the time series of the windowed data must be long and orthogonal.

Mathematically the DFT as applied to seismic data is expressed thus:

$$\mathbf{S\ (r\Delta f)} = \sum_{n=0}^{N-1} g(n\Delta t) e^{\frac{-2\pi i}{N} r\Delta f n\Delta t} \quad r=0,\ldots\ldots\ldots\ldots N\text{-}1$$

Where **N** is the number of time samples**, n** is the time sample index, **Δt** is the time increment, **r** is the frequency sample index, **Δf** is the frequency increment, **g(nΔt)** is the discretely sampled time signal, and **S(rΔf)** is the discretely sampled complex spectrum.

In spectral decomposition application, the Short Window Discrete Fourier Transform (SWDFT) has been demonstrated in bed thickness estimation and in validation of prospects. The underlying principle of SWDFT is from the convolution theory that states that a seismic data is a product of the convolution of the reflectivity series with the source wavelet added with noise. For a small window, a portion of the seismic trace is chosen as the zone of interest. This is the analysis window that may contain a few significant reflectors with amplitude at a particular location. The spectrum will be colored in the frequency domain. As shown in figure 2, when the small windowed trace is convolved with a band limited source wavelet such as a zero phase, in the

presence of noise the overall reflectivity is a band limited colored spectrum with wavelet overprint. This gives detailed information within that area and not random geological information.

Short Analysis Window spectral decomposition

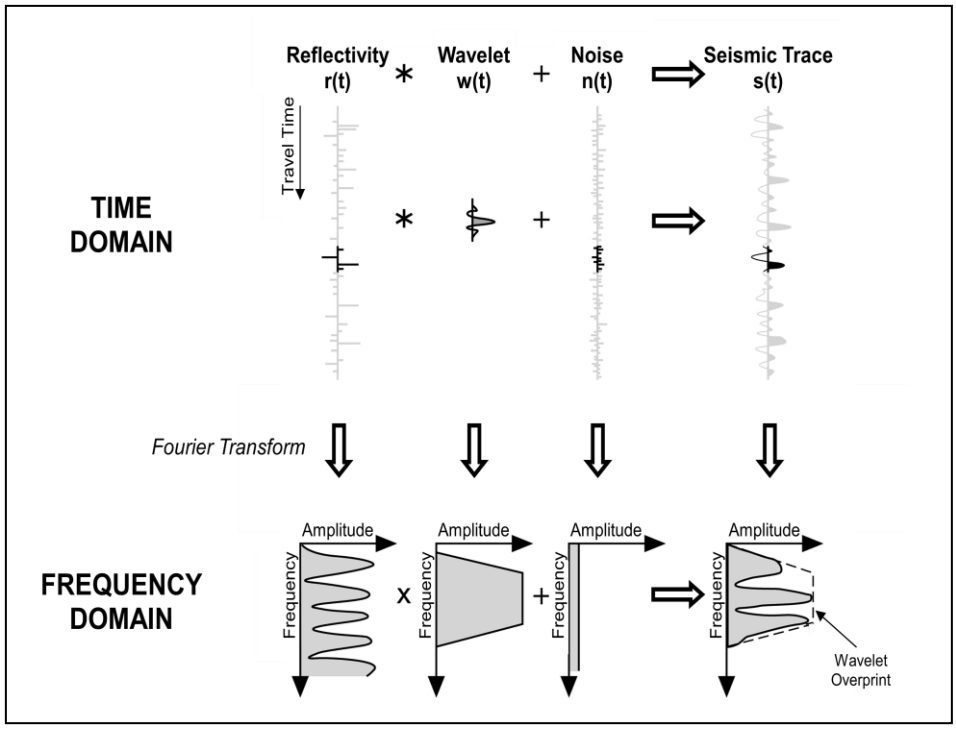

Figure 2. Short Window Discrete Fourier Transform (Partyka et al., 1999)

2.2.2 Wavelet Transform

Wavelet transform was introduced to analyze non-stationary signals with characteristic abrupt changes. An improvement that was made to curtail the limitation of the Fourier transforms. Jean Morlet, a French geophysicist in the 70's, worked in conjunction with

A. Grossman, a theoretical physicist who used an inversion based formula, to formulate this transform. They both felt that wavelets would provide a better time-frequency localization of signals. A wavelet is a small wave with short time impulse that tapers off quickly. Morlet considered the wavelet as a family of wavelet constructed from translation and dilation of a single function called the mother wavelet. The mother wavelet is defined here as:

$$\psi_{p,q}(t)=\frac{1}{\sqrt{P}}\psi\left(\frac{t-q}{p}\right)$$

Where p= scaling parameter (i.e. measures the degree of compression)

Q= Translation parameter which determines location.

Unlike the Fourier Transform that has sines and cosines as the basis functions, the wavelet transform uses the mother wavelet as the basis function, which is localized in frequency similar to sines and cosines. The localization which is also in time sharply contrasts to the Fourier transform. This dual localization of the wavelet renders most of the functions to be sparse-like favoring high level of accuracy when transformed into the wavelet domain. The basis functions of the mother wavelet are translated and shifted variations of the mother wavelet by varying the mother wavelet integers $\psi_{p,q}(t)$, which results in multi resolution both in temporal and frequency domain. Contraction gives better temporal resolution, while dilation gives poor frequency resolution. Multiresolution implies that gross outline of the feature can be observed with a large window, while sparse details are discerned with small window length. A major setback

for wavelet transform is that a wrong choice of wavelet in the analysis can give poor result compared to the Fourier transform. Therefore, prior understanding of the signal must be known in order to tweak the parameters to optimize the most suitable signal output.

2.2.2.1 Continuous Wavelet Transform

Like I noted earlier, the Fourier Transform is not suitable to analyze non-stationary signals. The signals are divided into segments before Fourier Transformed. This limitation is the basis for the formulation of the STFT. The physical phenomenon of Heisenberg Uncertainty principle affects virtually all transforms especially Fourier Transforms. The principle applied to signal analysis states that it is not possible to have both time and frequency information at a particular instant. One of them has to be forfeited for the other.

Continuous wavelet Transform (CWT) divides a signal into wavelets, and was introduced to curtail the limitation of the STFT by providing better resolution capabilities through the concept of multiresolution analysis. Multiresolution analysis (MRA), are designed to give better time resolution and poor frequencies at high frequencies and better frequency and poor time resolution at low frequencies (Polikar, 1996). CWT is computed in a similar way like STFT; the only difference is that the signal is multiplied by a wavelet instead of the window function in Fourier Transform.

Mathematically, signal analysis using CWT is expressed as:

$$\mathbf{CWT}_{(\tau,s)}=\frac{1}{\sqrt{S}}\int \boldsymbol{\psi}\left(\frac{t-\tau}{s}\right) x(t)d(t)$$

CWT $_{(\tau\text{-}s)}$ is the CWT scale decomposition, τ **i**s the translation parameter, **S** is the scaling parameter, ψ is the mother wavelet and **x(t**) is the signal. In geophysical applications, CWT has been demonstrated to be a powerful tool in decomposition of broad band wave field data using complex Morlet analyzing wavelet (Liner, 2010). Sinha et al., (2003) used Time-Frequency continuous wavelet transform to achieve optimum frequency resolution at varying frequencies. This circumvents the choice of a window length and provides high resolution at both low and high frequencies respectively. Chakraborty and Okaya (1995), show that CWT proffers solution to the resolution limitation of STFT.

2.2.3 Inversion

Reflecting energy recorded by receivers preserves earth models that educate us about the subsurface architecture. The motive for acquiring these models vary as many may want to study the whole earth structure from depths more than 100km. Others are more drawn to study contrasts in velocity as they could be viable indices to oil and gas accumulations. Either way, getting a true model of the subsurface is a significant step in knowing the earth accurately. This is known as forward modeling. Reconstructing the initial signal from the earth model is of itself the major role most geophysicists play to better know more about the earth structure. This concept is known as seismic inversion. Seismic inversion is a technique of perturbing the earth physical parameters from some set of observed seismic data. The perturbation is constrained to fit a set of parameters from a known model. Significant development has been made in seismic inversion in the past couple of decades. First we had the velocity inversion or what is known to some

people as travel time inversion or P-wave Tomography. This type of inversion generates a velocity depth earth model from the arrival times on the seismic traces at each receiver location. The travel time inversion is readily applied in earthquake studies and other areas of solid earth geophysics, but it has found applications in most processing suites for stacking and migration for better imaging purposes. Next is the inversion of amplitude or what is popularly known as acoustic impedance inversion. This inversion extracts amplitudes and arrival times from a seismic trace as a function of reflecting surfaces to model the geology for porosity and lithological prediction. Many kinds of acoustic impedance inversion have been developed among them are, band limited inversion, generalized linear inversion, simultaneous inversion and a host of others. Acoustic rock properties such as P-wave, S-wave, and density are usually the input parameters. Furthermore, another new dimension has taken to the series of inversion types. The inversion type is computed utilizing the frequency information mainly as a major input parameter, giving birth to spectral inversion. This term was coined to refer to inverting the frequency estimates derived from well data in an attempt to deconvolve the wavelet overprint on the reflectivity. This outputs a seismic data with high fidelity.

2.2.3. 1 Spectral Inversion

Spectral inversion is a sparse spike reflectivity series that is built on making geological rather than mathematical assumptions (Castagna et al., 2006). This concept reveals masked stratigraphy as well as thin beds that may be hydrocarbon bearing during production. The sparse spike reflectivity series produce high spikes in the vicinity of smaller spikes which are commensurate to the reflectivity of the earth. Spectral

inversion tries to enhance the resolution of the seismic data by removing details of wavelet overprint while boosting higher frequencies in the presence of noise. The Widess (1973) theory about thin bed proposes that the character of a seismic wave (peak/trough) doesn't change much in amplitude as a function of thickness but changes significantly with frequency. Below tuning, it becomes increasingly difficult to separate reflection coefficient from thickness. Hence, this gives the limit of visibility of that bed. However, this concept of Widess tuning model has its limitations as it is not applicable in practical cases. As observed by Tirado (2004), when he analyzed the odd and even pair reflection coefficient proposed by Widess's model, he observed that the amplitude increases then decreases. In actual sense, the magnitude of reflection coefficient should be a composite effect of the two reflections where the even part constructively interferes as thickness approaches zero, and destructively interferes for the odd part. According to Castagna (2004), that having a full understanding of the wavelet contribution from the even part produces a better resolution than the Widess's odd part. Partyka (1999) opined that the distance between the peaks and troughs of the spikes of a windowed seismic trace in the time domain gives us the bed thickness details. In general, spectral inversion is a conventional method that outputs a better image than the input seismic information. However, this method produces less reliable result as the level of noise increases.

2.2.3.1.1 Constrained Least Squares Spectral Attributes (CLSSA)

CLSSA is a spectral inversion algorithm that computes spectra decomposition. CLSSA inverts the Fourier series by inverting the sinusoidal kernels for a moving window. It would be

imperative to point out here that in Fourier transform, resolution is controlled by the window used, and the window used is its kernel function that runs from negative infinity to positive infinity. Inversion of the kernels produces the spectrum of the data within a window. The spectrum of the windowed data arises from the general rule of thumb that the sinusoidal basis functions must be orthogonal for a successful transformation. This has an effect of forfeiting the spectral resolution for time resolution. A way to correct for this is to solve directly for the Fourier series using the least squares solution within a window. This generates the spectrum of the data within a window. The inversion occurs where the window is centered on each time sample as the process is looped iteratively over the entire seismic trace. Samples that were not sampled can be properly sampled by this iterative process. Since spectral decomposition is a non-unique process, the sinusoidal kernel inversion may not be feasible as this depends on the constraints used, parameters chosen and assumptions made. CLSSA uses model and data to invert for the normal equations in time-frequency analysis (Puryear et al., 2012)

Part of the limitations of Fourier transforms and wavelet transform is that there is a tradeoff between spectral and temporal resolution in hydrocarbon detection and bed thickness estimation. The windowed DFT does not give the spectrum of the data within the window but the spectra of the windowed time series that has data within the window. By Fourier transform convolution theorem, this results in a spectrum that is the convolution of the true spectrum with the spectrum of the window. This spectral smoothing causes loss of frequency resolution and increase in bandwidth of the spectrum (Puryear et al., 2011).

Puryear et al, 2011, explained the concept of CLSSA forward problem as thus:

$$\mathbf{Fm=d}\text{.....equation 1}$$

Where **F**= the kernel matrix with real or complex sinusoidal basis

m is the model parameter otherwise referred to as unknown frequency coefficients in this case, **d** is the windowed seismic data. According to the algorithm, **d** is a segment of the complex seismic trace which has a real and an imaginary part.

$$\mathbf{d=d_r+d_i}\text{ equation 2}$$

Where $\mathbf{d_r}$ is the windowed segment of the real trace and $\mathbf{d_i}$ is the Hilbert transform of the seismic trace within a window. The number of columns in the kernel matrix F is chosen to complex sinusoids that truncate the window limit in the time domain.

$$\mathbf{F(t,f)=\cos(2\pi k\Delta fm\Delta t)+i\sin(2\pi k\Delta fm\Delta t)}\text{.....equation 3}$$

Here the number of columns and rows represents frequencies and the number of samples in the time window respectively. Usually the sinusoids are constrained to be correlated when they are not, the least mean square equation **F=md** above reduces to **m=F*d**. This is equivalent to the trace segment. Windowing the data correlates the elements of the kernel matrix, and the diagonals of the matrix are constrained by model weights, $\mathbf{W_m}$ and data weights $\mathbf{W_d}$, to obtain a unique solution. Model weights changes iteratively while the data weight remains constant in all iterations. This generates an ill-posed inverse problem to equation **F=md** from the weighted diagonal matrices $\mathbf{F_w m_w=W_d d}$. This equation is solved by applying the Tikhonov regularization to replace the equation with a well posed minimization problem. The Tikhonov regularization

parameter was reformulated by Portniaguine and Zhdanov (1998), which controls the stability and sparsity of the solution.

Heisenberg Uncertainty principle formulated as a fundamental theory in quantum physics, has also found applications in other areas of science. In its original form it is expressed in terms of observations and measurements. Gabor (1946) however relates this phenomenon to the area of signal processing and information theory. Uncertainty principle in mathematics is expressed as the standard deviation of position to the standard deviation of momentum and the Planck's constant. This has been reformulated in what is now accepted as Gabor's uncertainty principle, which states that deviations in frequency $\boldsymbol{\sigma}_f$ and deviation in time $\boldsymbol{\sigma}_t$ must be at least 80 millicylces.

$$\boldsymbol{\sigma}_f\boldsymbol{\sigma}_t \geq \frac{1}{4\pi} = 0.08 \text{ cycles}$$

In practical terms, the uncertainty principle says that it is not possible to represent a signal in time and frequency on the same plot. There is a tradeoff between frequency and time resolution. This brings an important issue in geophysics which is resolution. Two important concepts that apply to time and frequency resolution are localization and sampling. Localization in the time domain is based on the bandwidth and the tuning effects. It depends on how accurately we can interpret a reflectivity spike in the seismic. Localization in the frequency domain constitutes spectral leakage especially when the reflectivity is not a spike. For example the window length in Fourier analysis plays a significant role in the frequency resolution. On the hand, spectral side lobe and peak energy width controls leakage in the frequency domain during localization (Matt Hall, 2006). DFT and CWT are affected by resolution limitations in line with Heisenberg

uncertainty. CLSSA however has better frequency and time resolution, and hence good uncertainty product (Puryear et al., 2012).

2.3 Geology of the Stratton field

The complex reservoir heterogeneity in the Stratton field creates serious complications where lack of in depth understanding of the geologic variation may lead to incompletely drained or bypassed reservoir. Lateral variation in the geological complexity calls for the need to re-explore using modern technology for better precision drilling.

The Stratton field is among the most prolific gas field deposit in thin bed reservoirs, located in the Agua Dulce field in the Southeastern part of Texas (Hardage et al., 1994). Stratigraphically, the Stratton field is divided into two important formations. The Frio formation and the Vicksburg fault. The Vicksburg fault is a decollement surface characterized by antithetic faulting. The deformation that occurred during its deposition affected the Lower Frio Formation overlying it. The Oligocene Frio Formation is divided into three portions: The Upper, Middle and Lower formations. The Frio Formation is among the most prolific gas producing zones among the stratigraphic lithologies of the Cenozoic Gulf coast basin (Hardage et al., 1994). Frio Formation deposited via rapid sedimentation, has a thickness variation of 2000 ft near the Vicksburg fault, and greater than 9000 ft towards the Rio Grande embayment. The Rio Grande embayment is a discontinuous package of shale ridges, massifs and parallel strike slip growth faults (Galloway et al., 1982). The depositional setting below shows that the Frio Formation was formed from progradational deposits mainly siliclastics such as sand and shale.

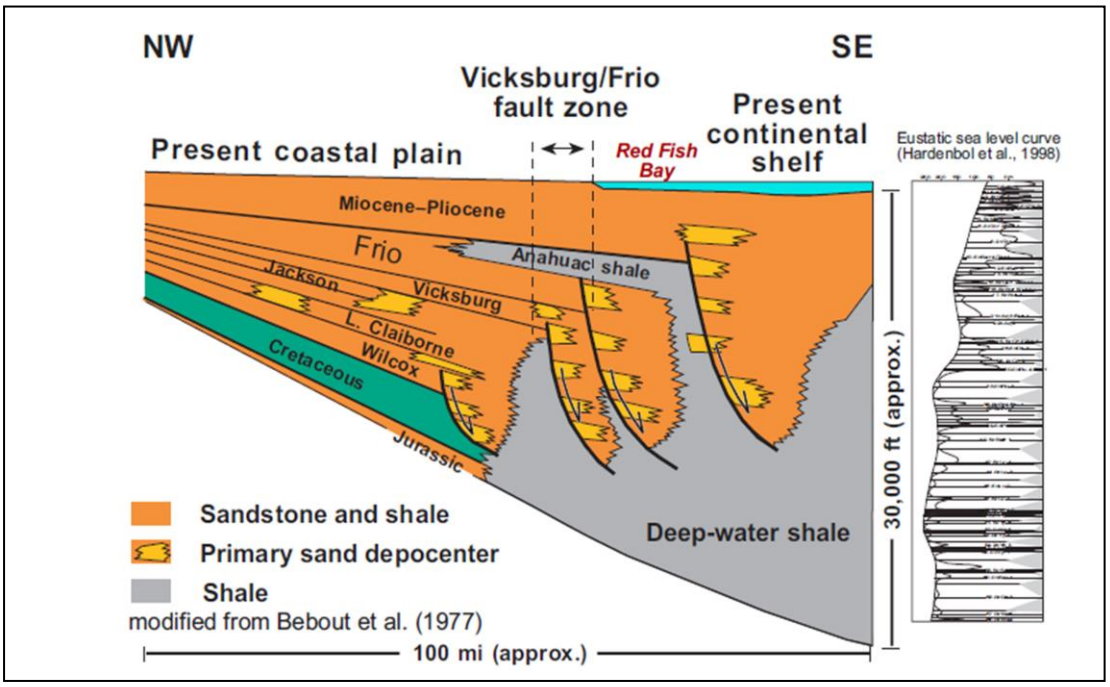

Figure 3 Vertical section through the depositional setting of the Stratton field (modified from Bebout et al., 1977)

The Frio Formation is subdivided into 10 gas plays based on regional and structural settings (Kosters et al, 1989). The gas plays in this field corresponds to the gas play FR-4 from Kosters et al, 1989, which is Fluvio/deltaic sandstones, ranked the third among the gas plays in Texas. Figure 4 shows the orientation of the gas play FR-4 in the Southeastern part of Texas. Among the nonassociated gas play in Texas, FR-4 is the largest with a cumulative production that exceeded 15 TCF in the past couple of decades.

\

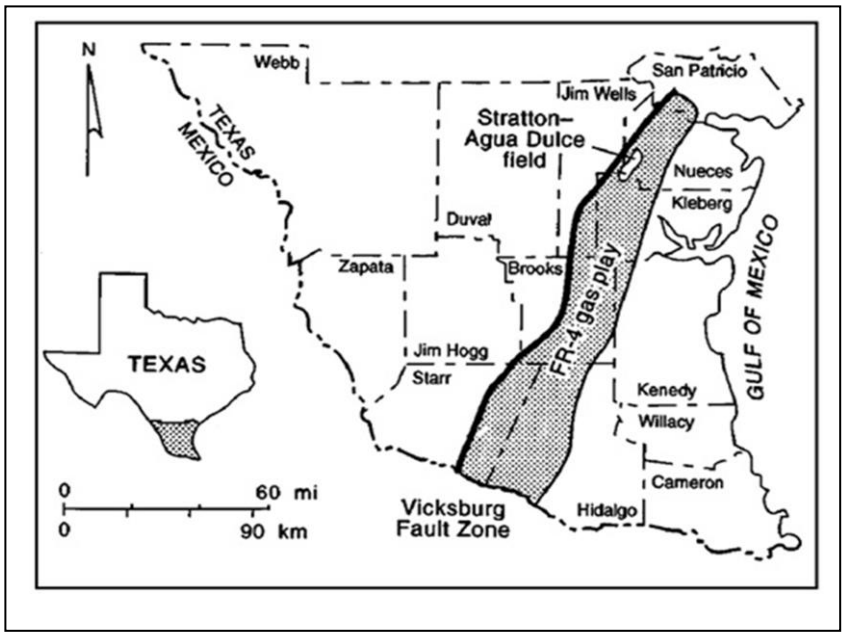

Figure 4 Regional setting of the FR-4 gas play with the location of the Stratton field (Hardage et al., 1994)

Structural and stratigraphic features that favored entrapment in this region include, faulted anticlinal closures, facies change and pinch outs (Koster et al., 1989). Majority of the reservoirs in the Stratton field are of fluviatile deposits located up dip of the Novias delta system (Figure 3). The Middle Frio Formation in this section of the field is characterized by flat lying geology, and the likely trapping mechanism would be more stratigraphic than structural.

2.3.1 Stratigraphy of the Frio Formation

The middle Oligocene Frio formation was formed during the Catahoula depositional episode (Galloway, 1977). The Frio deltaic sandstone play FR-4 is among the most prolific gas plays in Texas, and the trapping mechanisms are reservoir pinch out, facies change and anticlinal closures (Kosters et al., 1989). The 3D seismic data used in this

work is obtained from the Stratton field, which is at the northern limit of the FR-4 gas play. Analysis of well logs from the field reveals that the Frio formation consists of multiple stacked pay sandstones within a vertically stacked reservoir system labeled as: B, C, D, E, F series (Hardage et al., 1994). Borehole analysis from well logs reveals that the sandstones are amalgamated channel infill deposits ranging from 10-30 feet in thickness, with some splay sandstone. The channel fill have either a blocky or upward fining SP log profile, while the splay deposit shows a classical upward coarsening textural profile.

The Upper Frio (3,800 to 4,500 ft.) consists of laterally-continuous sandstone interbedded with mudstones which are about 40-80 ft thick. This portion of the Frio Formation witnessed retrogradational wave dominated deltaic system and progradational phase of stradplain system (Kerr, 1990). The middle Frio Formation (4500 to 7000 ft) consists of channel fill and crevasse splay and well-developed levee sandstones that are slightly sinuous and form part of a fluvial system (Jirk, 1990). From Jirk (1990) and Kerr and others (1992), both stated that the depositional environment of the middle Frio consist of the following facies: channel fill facies that are laterally accreted point bar deposits which are about 15 to 45 ft. thick and moderately straight with a width between 2,000 to 2,500 ft wide. Splay sandstone facies are fan shaped and coarsen upward. They are about 10-30 ft thick next to the channel and extend to about 2-3 miles before pinching out. The porosity of the splay is between 5-30%. The last facies type is made up of levee and flood-plain mudstone. The levee facies are lateral to channel fills and consists of mudstones, siltstones, and are about 100-500 ft. wide. The

flood plain mudstone consists of intercalations of clay, silt and sand having low porosity, and not well developed parallel laminations.

2.4 Well Tie

The BEG Stratton field data set consists of 21 wells with no check-shot survey or sonic log. There is however a VSP survey for well 9, which was the well I used for the seismic calibration. 3D seismic interpretation begins with calibration of wells to surface seismic data. The sole objective is to match the well logs measured in depth to surface seismic measured in time, to simulate the subsurface geology by relating the seismic reflections to the stratigraphy. By far, sonic log gives us a hint about the transit time of a wave in a lithology carrying with it signatures of fluid saturation or other rock properties. However, when this is absent, it becomes imperative to generate a pseudo-sonic log from a suite of nearby logs using any of the popular rock physics transforms such as Gardner or Faust's equation. The velocity information may not be perfect like a real sonic but having a little of something is better than not having anything at all. The suite of well logs in the BEG Stratton data set has no sonic log, so generating a pseudo log from density using the Gardner's relation gave me something unreliable to work with, as there was huge disparity in the depth values. However, using the Faust relationship to generate the pseudo-sonic log from resistivity log produced a more reliable result as the depth values were accurately placed. Having two important logs of density and pseudo sonic, I modeled the subsurface reflectivity by convolving them with a Ricker wavelet to generate a synthetic seismogram. The Ricker wavelet is notable for its preference in modeling as it provides superior vertical resolution. I generated the Ricker for this well

tie using the dominant frequency from the data, which also filters off the low frequency reflections below the dominant frequency. Figure 5 shows the well tie and the wavelet used for modeling the reflectivity. To place accurately where each reflection is on the subsurface, I had to match and shift the reflectors on the synthetic to match the well logs until the peaks and troughs are aligned, or the energy in the main lobes appear to be so, even though the energy sometimes are in conflict on the synthetic from what's on the seismic. This is part of the limitations of modeling using a pseudo sonic logic. An anomalous region of increase in impedance was observed on the resistivity, induction and sonic log from 1440 ms to 1430 ms in a coarsening upward sequence manner. Correlation coefficient of the simulation of seismic to real geology is at 64.5%, which is more than fair. This zone corresponds to a trough on the seismic. Guided by this, I tracked the anomaly to display a splay channel-like stratigraphic sand body which is gas charged. This is a channel in-fill sandstone deposits with splay deposits. I will use the term 'D' sand series interchangeably, with channel in-fill sandstone with splay deposits in this work. The term adaptation is because this area of interest falls within the 'D' sand series identified by Hardage et al, 1994, to be among the prolific sandstones reservoirs of the middle Frio formation.

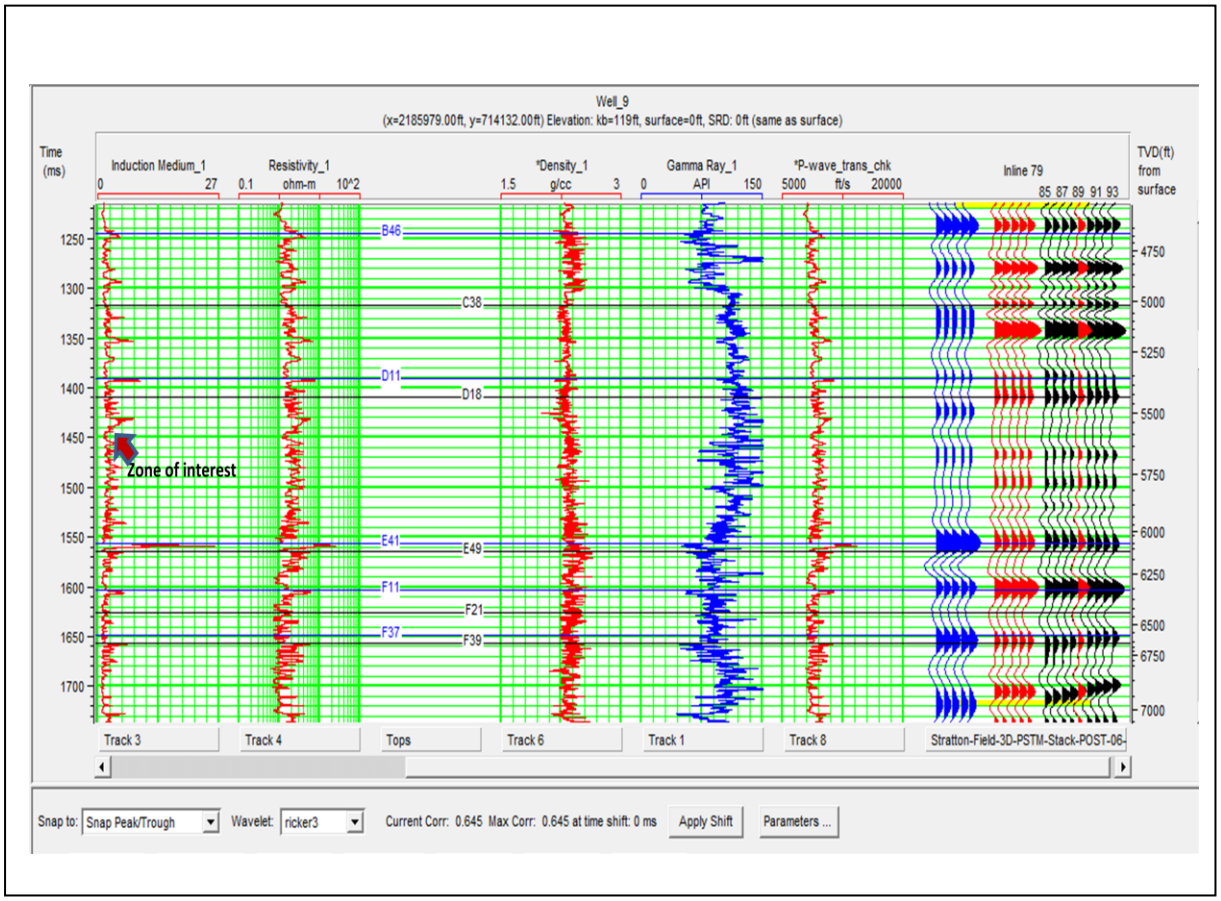

Figure 5. Well tie with zone of interest indicating a coarsening upward sand sequence

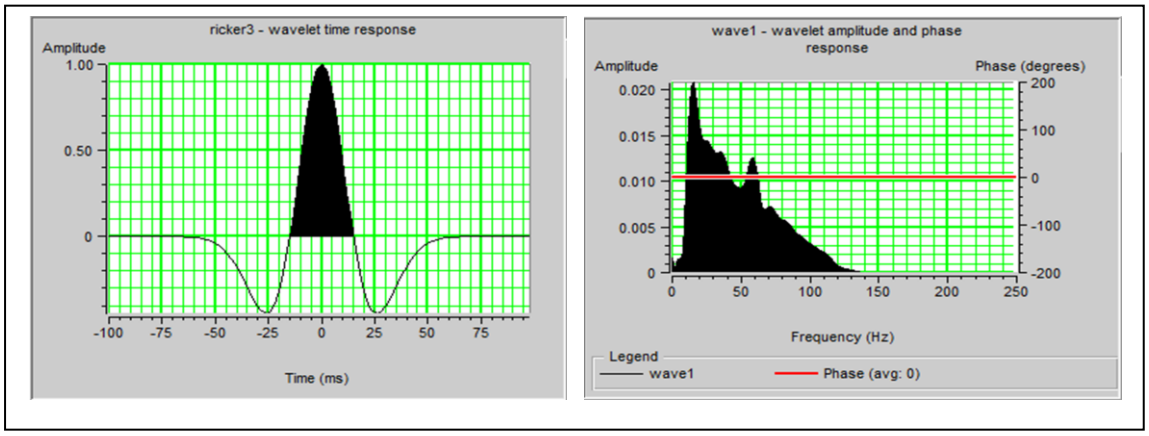

Figure 6. Ricker wavelet created and its associated amplitude spectrum

CHAPTER THREE

SPECTRAL DECOMPOSITION INTERPRETATION

In the previous chapter, I gave a glimpse about the theory underlying the two most popular transforms that computes time-frequency analysis. I also brought to the fore the concept behind a new technology which is an improvement upon the classical Fourier transforms. Nevertheless in this chapter, I am going to talk about the method I adopted to make a comparison between the three algorithms as they apply to real seismic data in delineation of subtle stratigraphic features.

Spectral decomposition is time-frequency localization in interference patterns from thin layers, having information in the frequency domain about bed thickness. Seismic interference can be categorized into two (Jakosky and Jakosky, 1951). The first category of interference is that observed from a reflector that has a frequency located in the frequency spectrum but the reflection is outside the desired reflecting band. The reflections are lower than the reflections of interest and enhancement is achieved by using a high-pass filter. The second type of interference is between closely spaced reflectors, or between a reflection and interference within the reflecting band spectrum. A geological scenario that gives rise to this kind of inference is in stratified layers with reflection coefficients of similar amplitudes occupying a narrow portion in the frequency spectrum. The contributing effect of interference patterns not only to the resolution of the seismic, but also the reservoir economics of a basin cannot be overemphasized. Thin

layers of porous sandstones encased in a hard material which are significant to overall reservoir volumetric, are usually bypassed during reservoir characterization as their amplitudes are masked by stronger reflections.

3.1 Method

Horizon maps are by far the most effective way to display a 3D architecture of the subsurface in a 2D map view. The maps are obtained from tracking an event corresponding to amplitudes or structure of interests. In my work, I mapped an amplitude event representing coarsening upward channel in-fill sandstones with splay deposit at a level as indicated from my well tie. I tracked this event at an inline and crosslines spacing of 1 interval. The reason for this is to create a closely spaced cell grid to get a detailed geological interpretation. To achieve part of my objective, I had to transform this horizon information at a particular time to the frequency equivalence using different spectral decomposition algorithms as described above. I import the original seismic data into the program specifying a window length for each computation. Running windows of 20 ms and 40 ms are used here respectively. The term running windows and analysis windows will be used interchangeably in this write up to mean the same thing, that is the size of the of the spectral decomposition window that's believed will aid to capture features below resolution. Thin layers smaller than a given window size may not be captured. The products from this horizon transformation are amplitude and phase volumes ranging from 1-80 Hz. The amplitude spectrum of the data is from 3-120 Hz, beyond 80 Hz the amplitude spectrum begins to taper off into the background. Since this work is focused on stratigraphic visualization, I chose to concentrate on the

amplitude volumes associated with each frequency, as they are commensurate to the frequency phenomena of ''tuning in and tuning out'', characteristic of sand bodies above or below seismic resolution.

3.2 Results

Seismic data is broad bandwidth information of the subsurface that contains obscured geologic details which remains hidden to many interpretation methods. There is a proliferation of different attributes today in the quest to better image and characterize a reservoir. These varieties of attributes are built to be sensitive to a particular reservoir feature. Spectral decomposition utilizes the frequency component when the bandwidth of the seismic data is dissociated into discrete components to reveal subtle features obscured by interference patterns. Here I will compare the fidelity capabilities between DFT, CWT and CLSSA.

Figure 7a shows instantaneous amplitude highlighting a channel in-fill with splay stratigraphic package that is gas charged. The bright spot at the northern most part signifies a gas charged channel in-fill sandstone that is relatively thicker than the other areas. Figure 7b shows a vertical well section showing a similar lateral stratigraphic orientation like the 'D' sand series. This is from F37 reservoir after Hardage et al, 1994. Using running windows at 20ms and 40ms, I transformed the horizon into a series of spectral maps. This is so because different beds require a particular frequency that will excite the waveforms to reveal subtleties.

Figure 8 shows a comparison between the seismic amplitude and a series of frequency maps for CLSSA. Figure 8a shows the amplitude map, white arrows in figure

8b highlights enhanced subtle sand bodies absent from the seismic amplitude map. 10 Hz is where the dominant energy is as later frequencies reveals less of the high amplitude sand bodies on the map. This implies that as the frequency increases, the resolution decreases for the CLSSA as observed in this case. The black arrows in figure 8a, points to sandy features on the amplitude map that were suppressed in the frequency maps. These features could be noise or sand bodies with frequencies on the high end of the frequency spectrum.

In figure 9, I made a comparison between amplitude map and the DFT frequency maps. Here, there is a stark similarity between the amplitude map and the features on the frequency maps. Among the obvious difference between this attribute and the previous one is that at 10 Hz, which is where the dominant energy is, there is a tuning out of the stratigraphic amplitude. As the frequency increases, the features tune in as observed in figure 9c and figure 9d. This implies that as frequency increases, resolution increases. The frequency increase did not enhance the interpretation as the best spectral map looks like the amplitude map. This takes us back to the behavior of DFT within a spectrum of a windowed data. The spectrum displayed by DFT in this case will be that of window containing the data, hence forfeiting spectral resolution for temporal resolution.

Figure 10 presents another attribute comparison between seismic map and the CWT attributes. At dominant frequency, the CWT does poorly as there is smearing of amplitude of the reflections. At higher frequencies the features completely disappears leaving only the low amplitude features. The reason for the poor performance of CWT in

this case could be that the Morlet wavelet used as window function may not be the best wavelet in this case. More confidence could be ascertained if other wavelets are used.

Figure 11 shows comparison between the three attributes at dominant frequency. CLSSA in figure 11b shows an enhanced display of the feature than the rest at this window length. A likely reason for this could be the iterative nature of the data within a given window during its computation. There is tuning out of the gas charged sand bodies on the frequency map for DFT, while there is complete amplitude smearing, obliterating the feature on the CWT. To revisit the phenomenon of Uncertainty principle here, CLSSA has better uncertainty product than DFT and CWT. A logical reason could be hinged on the behavior of the methods to the spectrum of the windowed data. CLSSA gives the spectrum of the data within the window, while DFT gives the spectrum of the window containing the data. CWT is not window dependent, as the cross correlation between the seismic trace and the wavelet requires no window length.

Figure 12a shows a line spectrum at a time value extracted from the bright spot at the middle of the channel in-fill on the seismic section. A trace is extracted, decomposed and plotted as a function of time and frequency (T-F panel) to ascertain their vertical resolving capabilities. The three attributes are placed side by side as shown. In the T-F panel of the CWT, there is a poor time resolution at high and low frequencies. At high frequencies, there is a loss of signals as the events are smeared towards the low frequency trend of the spectrum. At 1464 ms, the bright spot event is smeared appearing low in magnitude. In the DFT panel, the event at 1464 ms appears as a weak superimposed doublet of a peak over trough events notched out at 40 Hz. The

notches in time on the DFT panel occur approximately at 40 Hz and 70 Hz. If the notch periods are correct, then the time thickness of the channel in-fill will be about 12.5 ms. DFT smears the energy across the spectrum and treats the channel in-fill as a thin layer with superimposed doublets impressions on the frequency panels, making the time and frequency resolution to be very poor. On the CLSSA panel at 1464 ms, the event is well resolved in time and frequency that terminates beyond 40 Hz. CLSSA did not resolve the channel in-fill as a doublet; rather it resolves it better as sharp features. Apparently the notch frequency observed on the DFT at 40 Hz appears beyond that on the CLSSA panel. DFT gives erroneous notch frequency. Notch patterns absent on CWT are present on both the CLSSA and DFT panels.

A time slice extracted at 1464 ms passing through the bright spot in 1D creates a 2D relationship between the frequency range of the data and the normalized amplitude spectrum. In figure 12b, the spectrum of the CLSSA concentrates all its energy between 10-50 Hz with a steep slope. Concentration of the energy in this range of frequency explains why the spectral resolution decreases as frequencies increases. Also the notch frequency is at 50 Hz which shows that the bed must be thinner than what the spectrum of DFT shows. DFT spectrum on the other hand, experiences a drop in amplitude as frequency approaches the dominant frequency. At 11 Hz and above, the spectrum picks up energy until it is notched out at 40 Hz and 70 Hz respectively. The frequency range is narrow and less steep compared to CLSSA. CWT amplitude spectrum is smeared at the low frequency end of the spectrum.

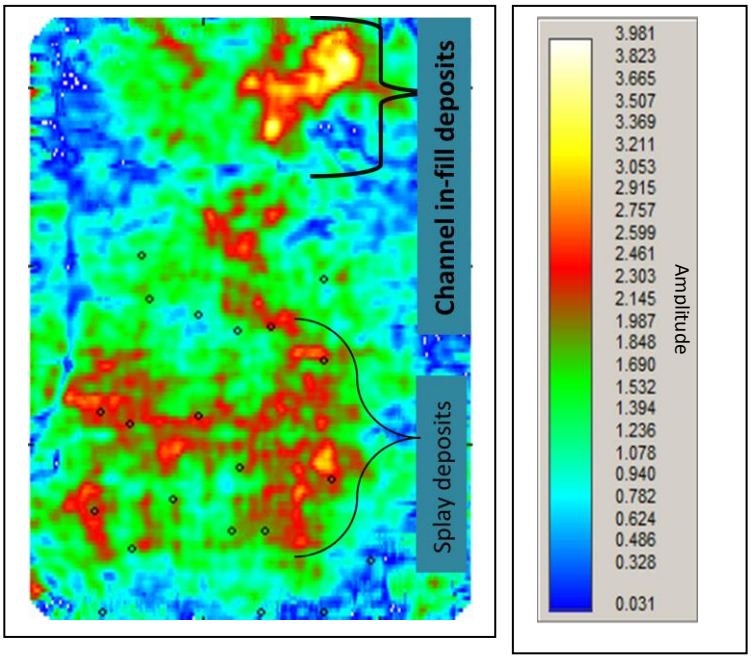

(a)

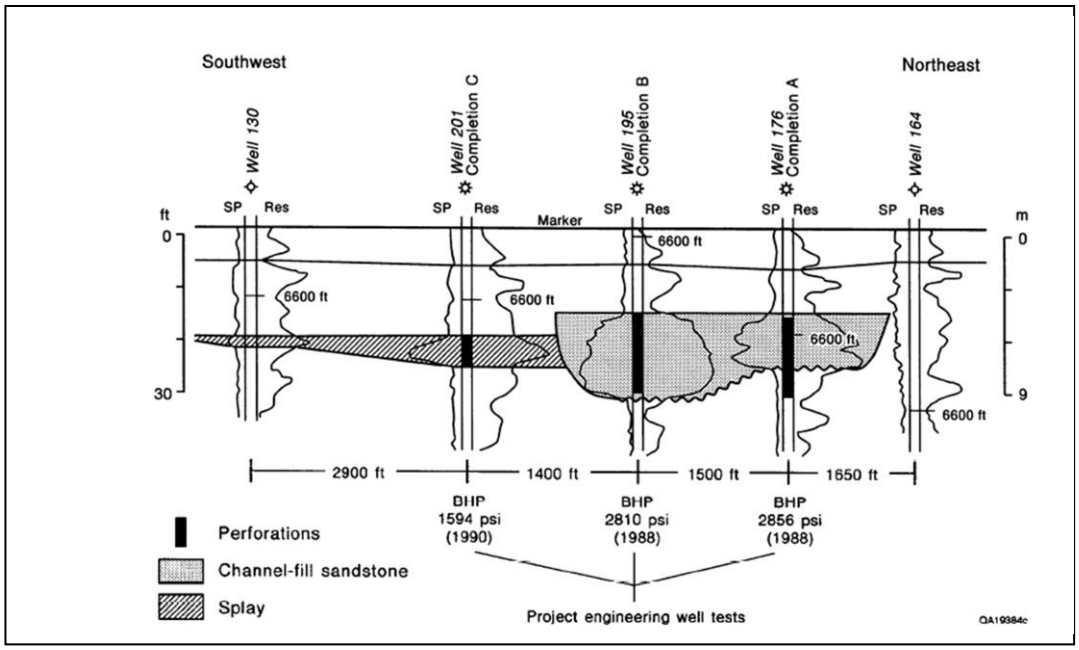

(b)

Figure 7(a) Instantaneous amplitude showing channel in-fill sandstone and splay deposits. Dots on the map are wells located in the area (b) Reservoir F37 from vertical well section having similar lateral stratigraphic orientation as the 'D' sand series (from Hardage et al, 1994).

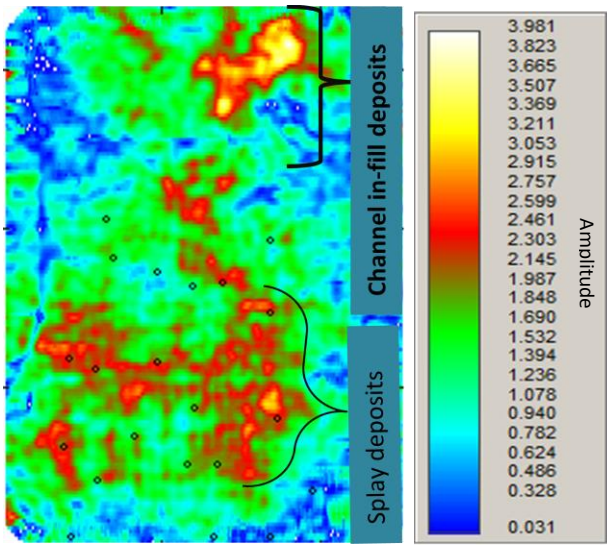

(a) SEISMIC INSTANTANEOUS AMPLITUDE

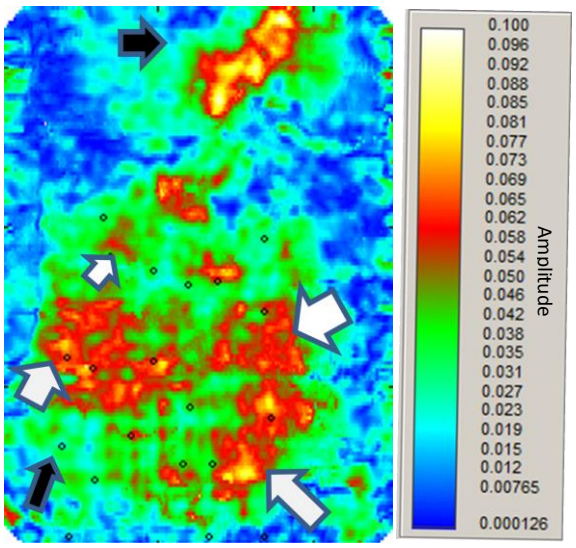

(b) CLSSA 10 Hz

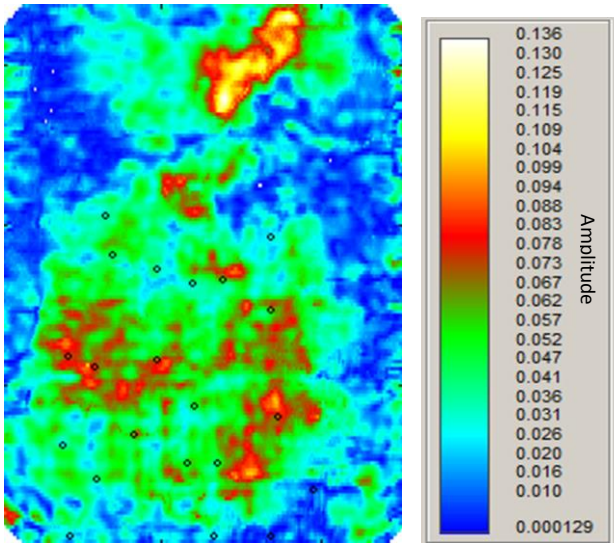

(c) CLSSA 15 Hz

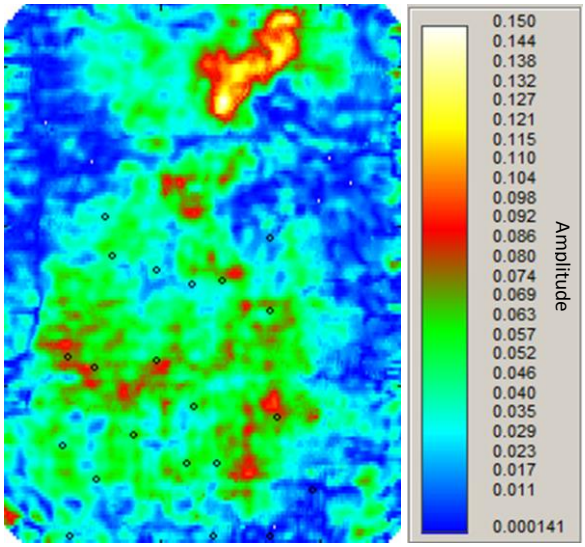

(d) CLSSA 20 Hz

Figure 8. Comparison between seismic and frequency attributes display. (a) Seismic amplitude map showing channel in-fill deposits. (b) CLSSA at 10 Hz. White arrows pointing to enhanced features absent on the seismic amplitude. Black arrows showing features present on the seismic but absent on the frequency attribute maps. (c) CLSSA 15 Hz (d) CLSSA 20 Hz. Frequency volumes were generated at 40 ms analysis window. Notice as amplitude decreases as the frequency increases.

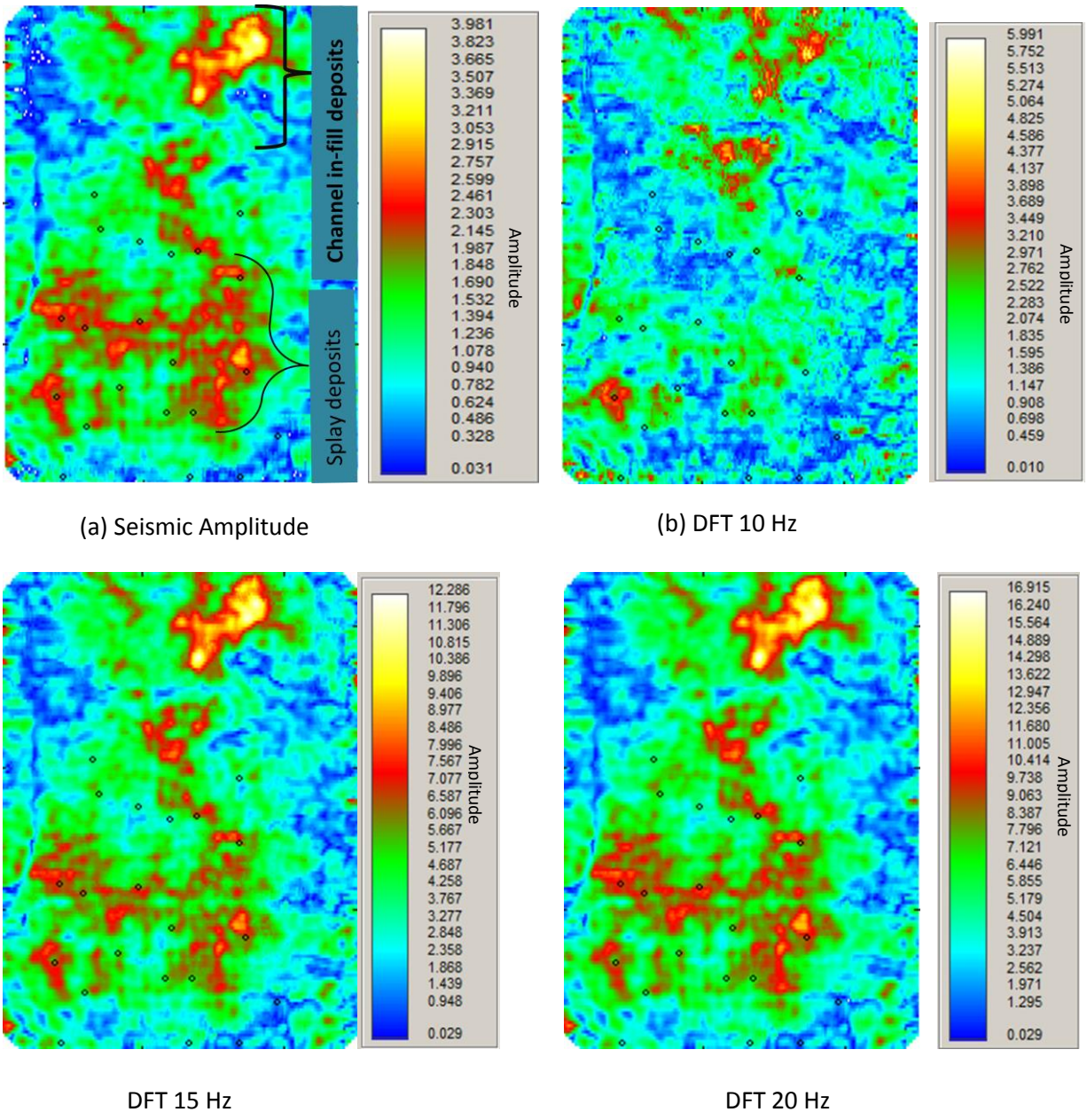

(a) Seismic Amplitude

(b) DFT 10 Hz

DFT 15 Hz

DFT 20 Hz

Figure 9. Comparison between Seismic amplitude map and DFT attributes. (a) Seismic Amplitude map (b) DFT 10 Hz (c) DFT 15 Hz (d) DFT 20 Hz. DFT analysis window length is 40 ms. Notice how there is obliteration of the feature at peak frequency of 10 Hz.

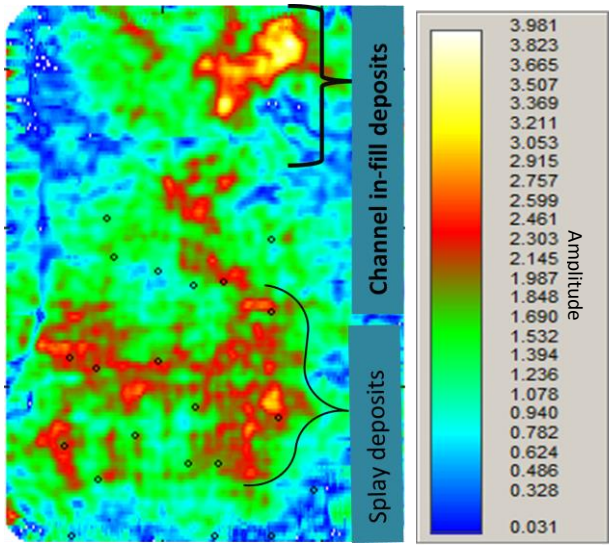

(a) Seismic Amplitude

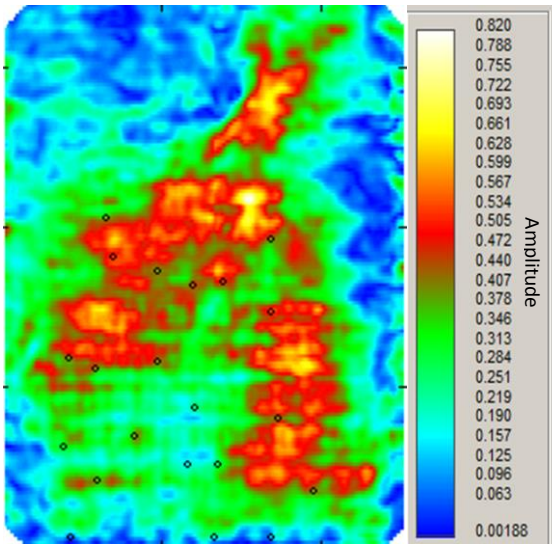

(b) CWT 10 Hz

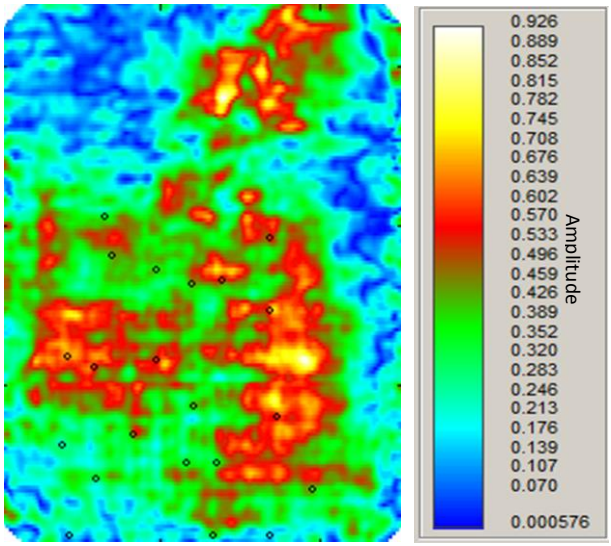

(c) CWT 15 Hz

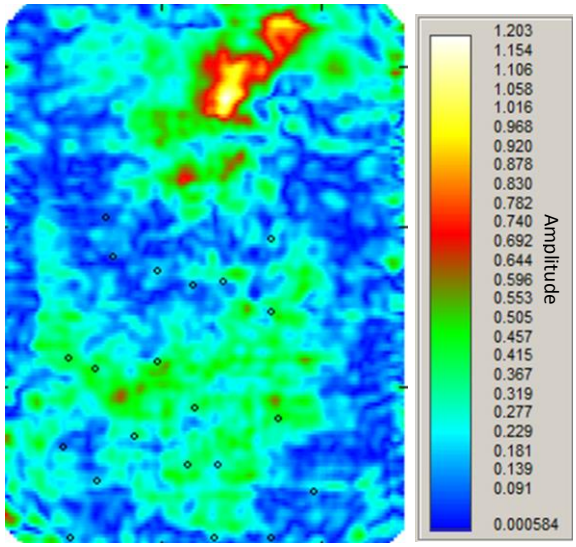

(d) CWT 20 Hz

Figure 10. Comparison between Seismic amplitude and CWT frequency attributes. (a) Seismic amplitude map (b) CWT 10 Hz (c) CWT 15 Hz (d) CWT 20 Hz. CWT is not window dependent.

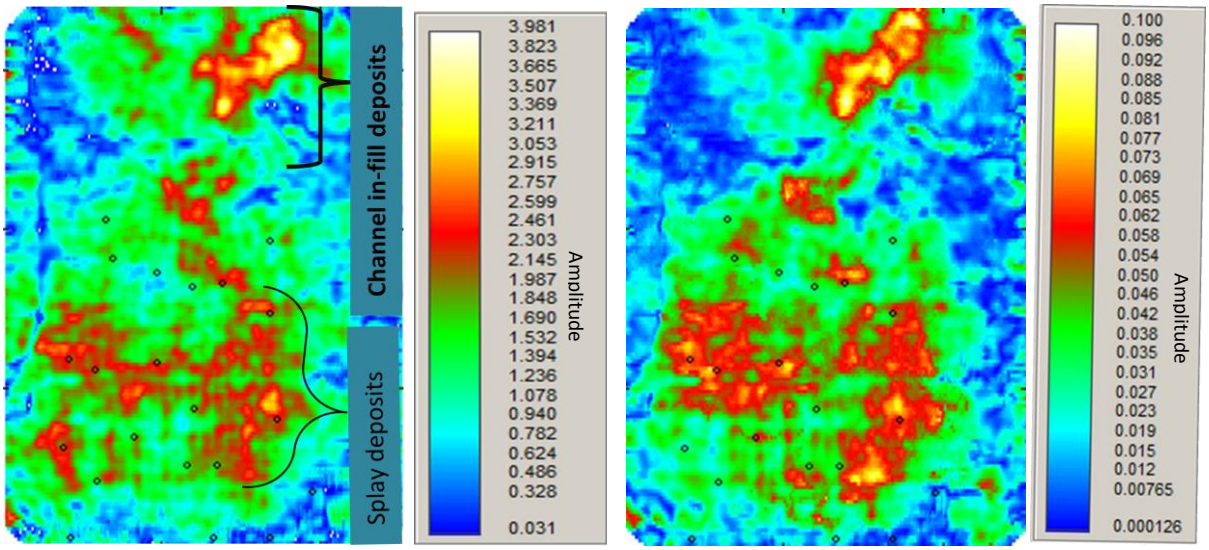

(a) Seismic amplitude (b) CLSSA 10 Hz

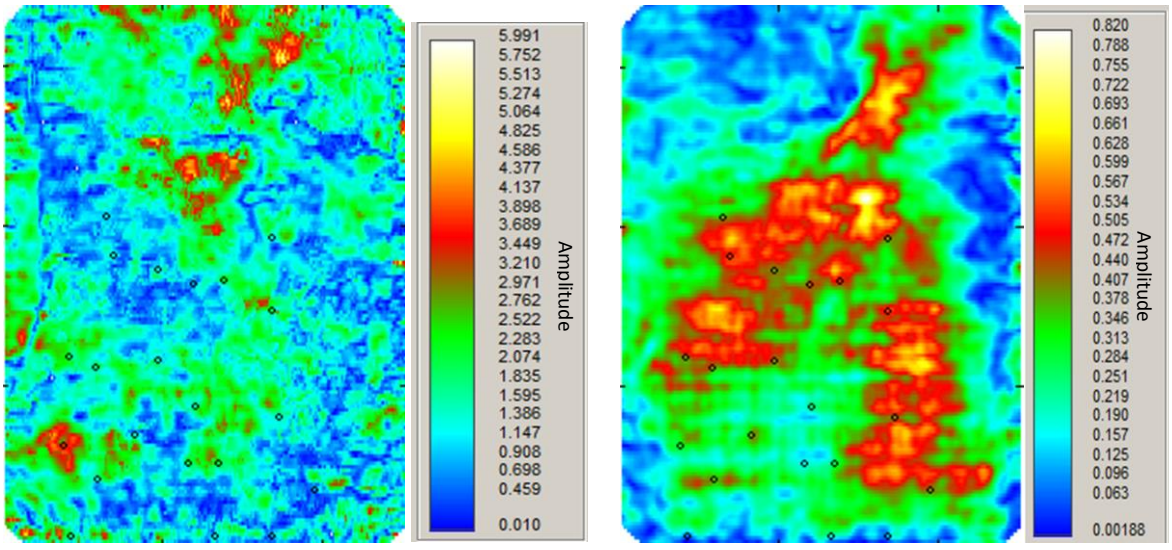

(c) DFT 10 Hz (d) CWT 10 Hz

Figure 11. Comparison between seismic amplitude and peak frequencies for the three attribute volumes highlighting the 'D' Sand series. (a) Seismic amplitude map (b) CLSSA 10 Hz

(c) DFT 10 Hz (d) CWT 10 Hz.

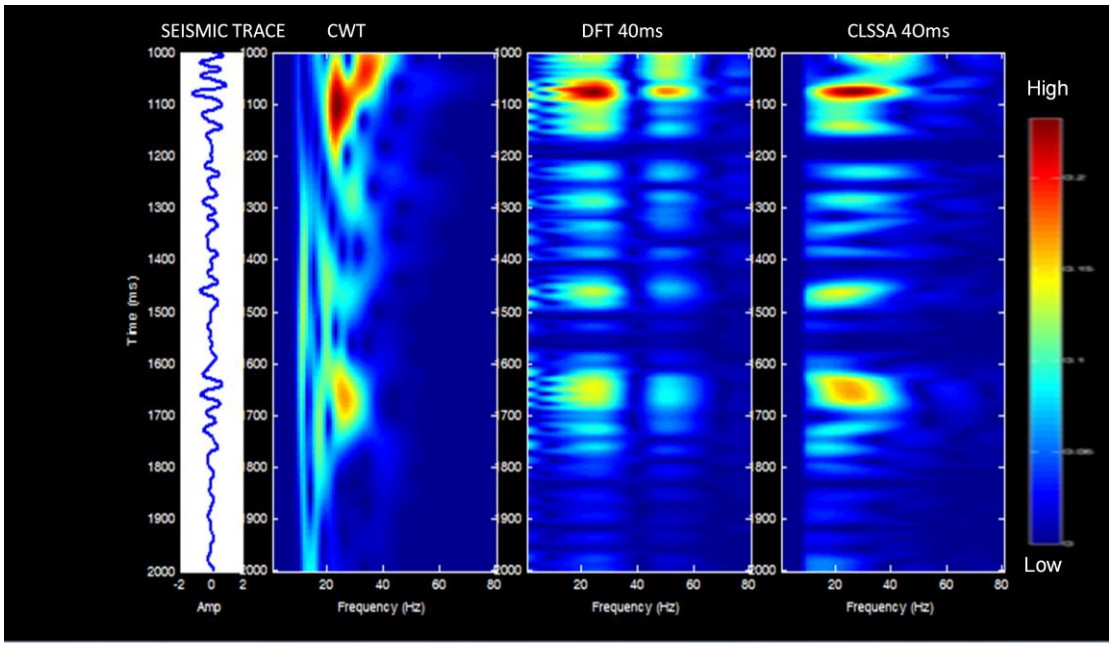

(a)

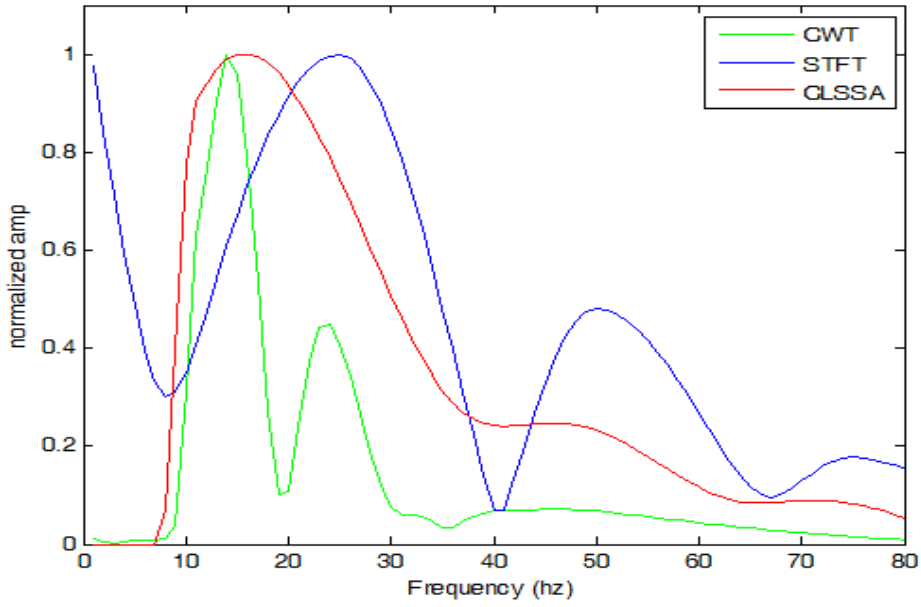

(b)

Figure 12. (a) Time-frequency panel of a trace extracted from the channel in-fill deposit at 1464 ms. See how the three methods try to resolve the trough event at 1464 ms on the trace. Analysis window for the trace decomposition is 40 ms (b) Line spectrum sliced at 1464 ms to show the shape of the frequency spectrum relative to normalized amplitude at that event

Figure 13 shows the time-frequency panel of a trace extracted at the same channel in-fill deposits at 1464 ms. CWT smears the energy across its spectrum exhibiting poor time and frequency resolution. DFT gives a notch pattern at 20 Hz and there appears some energy appearing on the low frequency reflectors. This could be noise or interference energy outside the spectrum, giving a poor frequency resolution. In the time domain, the superimposed doublets observed in the 40 ms window are now resolved into three thin layer reflectors. DFT sees the channel in-fill deposits as thin layers separated in time. On the CLSSA panel, the feature exhibits sharper frequency and improved temporal resolution. The feature is notched out at 50 Hz. Thus it becomes important to conclude that CLSSA will produce better spectral resolution maps of the stratigraphic feature than DFT and CWT.

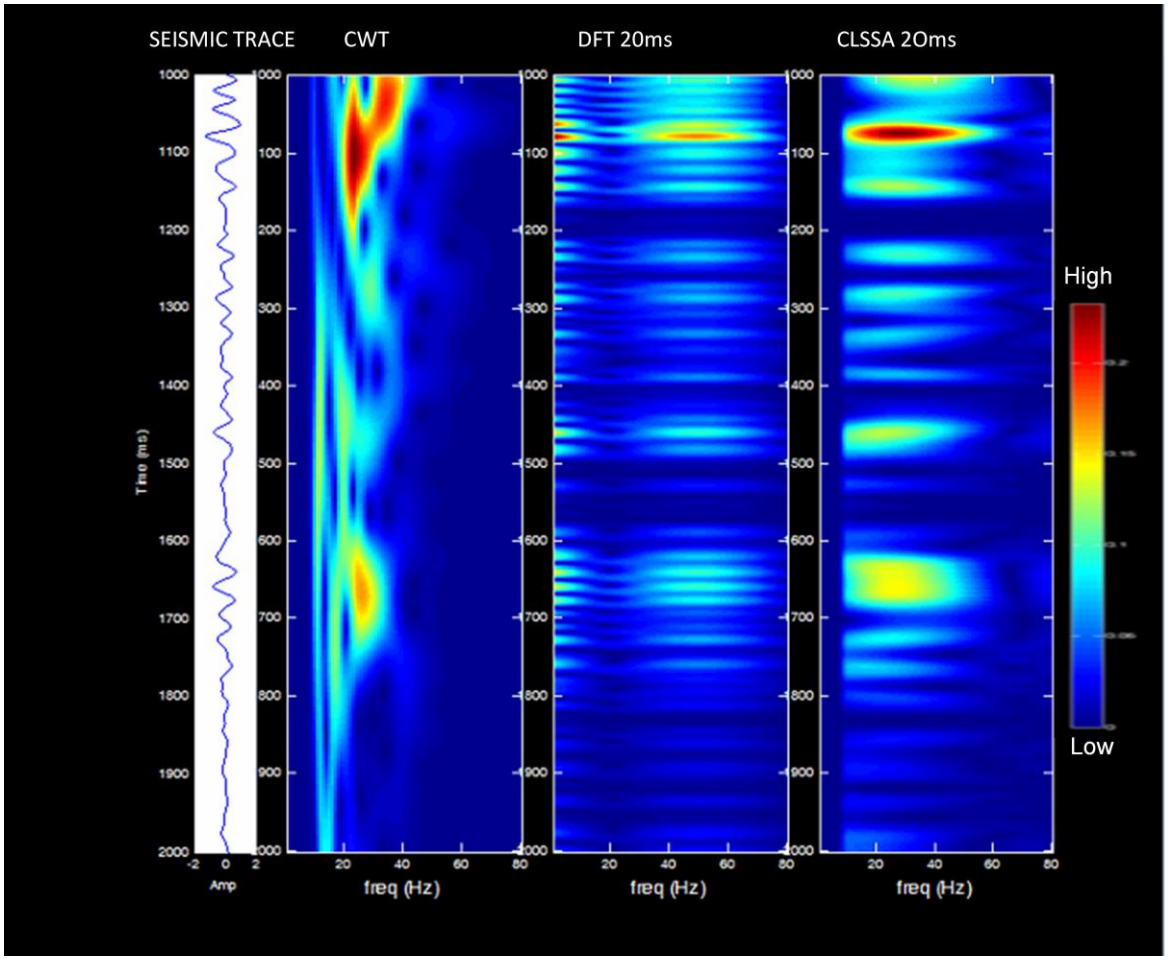

Figure 13. Time-frequency panel of CWT, DFT and CLSSA from a decomposed trace extracted from the channel in fill deposit at 1464 ms.

When I halved the window size to 20 ms, the spectral map of CLSSA at 10 Hz shows the white arrows indicating enhanced stratigraphic bodies absent on the seismic. Figure 14c shows that at 15 Hz and above, there is gradual tuning out of the features on CLSSA. This means that the peak frequency at this window size falls rapidly to almost that of the seismic than at 40 ms window size. Figure 15b-d, shows the spectral maps of DFT at 20 ms window. The phenomenon of tuning in at the peak frequency is antithetical to what is observed at 40 ms analysis window. Here the peak frequency decrease from low frequency, and becomes completely obliterated at high frequency of 20 Hz. CWT will

not be displayed here because it is not window dependent. It wouldn't change the spectral map interpretation whether at small or large windows; it will always be plagued with interference patterns irrespective of the frequency. Figure 16 shows a comparison between all the attribute volumes. Notice how the CLSSA resolves subtle features absent on the seismic than DFT and CWT.

From the above results, it would be appropriate to conclude that irrespective of the thickness of the bed here and the analysis window, CLSSA resolves the beds better. CLSSA exhibits better Heisenberg uncertainty product both at 40 ms and 20 ms than DFT that shows inconsistencies in locating the peak frequency and notch location. CWT adds nothing to the interpretation as lots of amplitude smearing in both time and frequency domain.

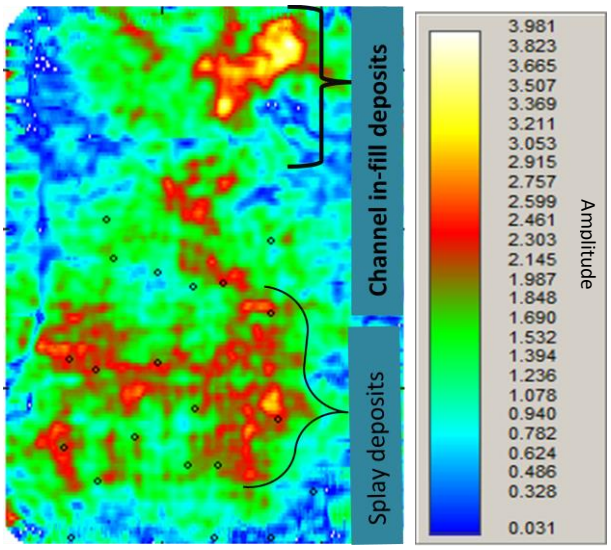

Seismic Amplitude

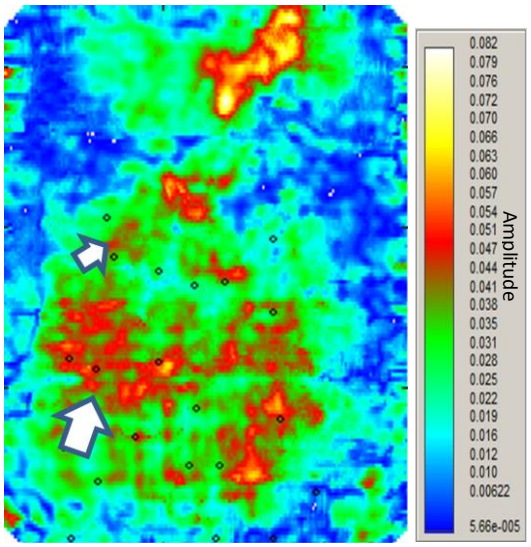

CLSSA 10 Hz

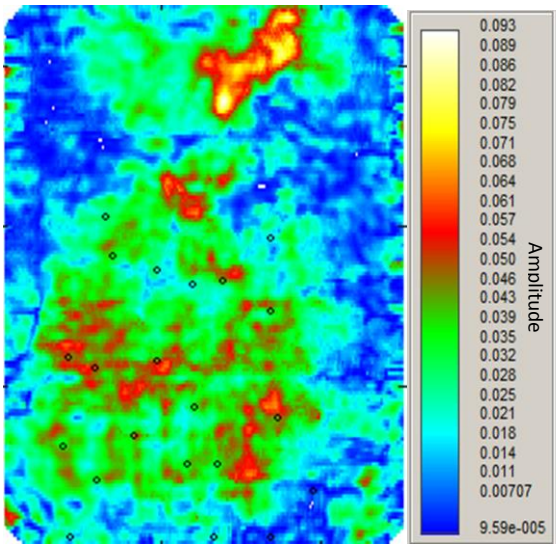

CLSSA 15 Hz

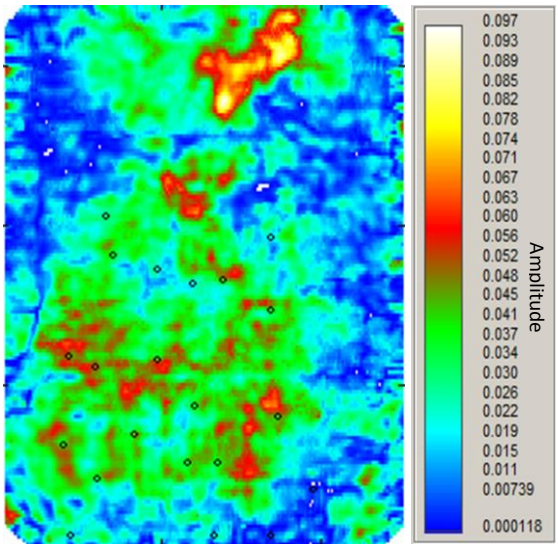

CLSSA 20 Hz

Figure 14. Comparison between seismic Amplitude and CLSSA spectral maps at 20 ms analysis window.(a) seismic amplitude map (b) CLSSA 10 Hz. White arrows show enhanced features on CLSSA that is absent on the seismic amplitude map. (c) CLSSA 15 Hz (d) CLSSA 20 Hz. At this analysis window, spectral amplitude of the feature decreases with increase in frequency.

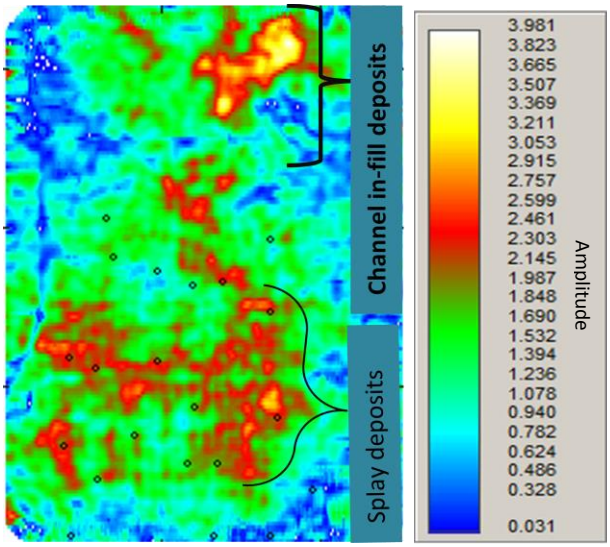

Seismic Amplitude

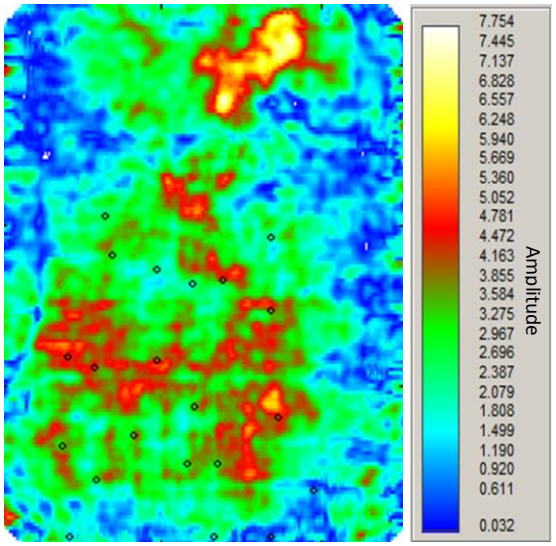

DFT 10 Hz

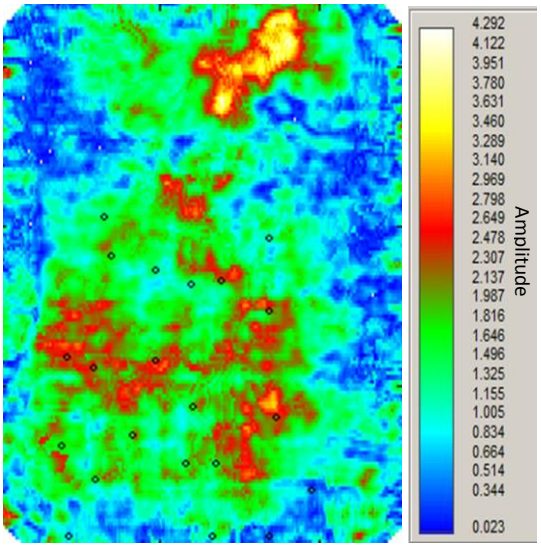

DFT 15 Hz

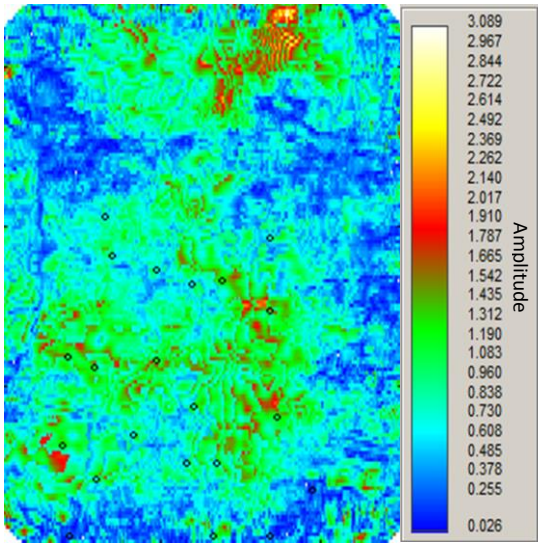

DFT 20 Hz

Figure 15. Comparison between DFT spectral maps at 20 ms window and Seismic amplitude. (a) Seismic amplitude map (b) DFT 10 Hz (c) DFT 15 Hz (d) DFT 20 Hz. Notice the similarity between DFT at peak frequency of 10 Hz and the seismic amplitude.

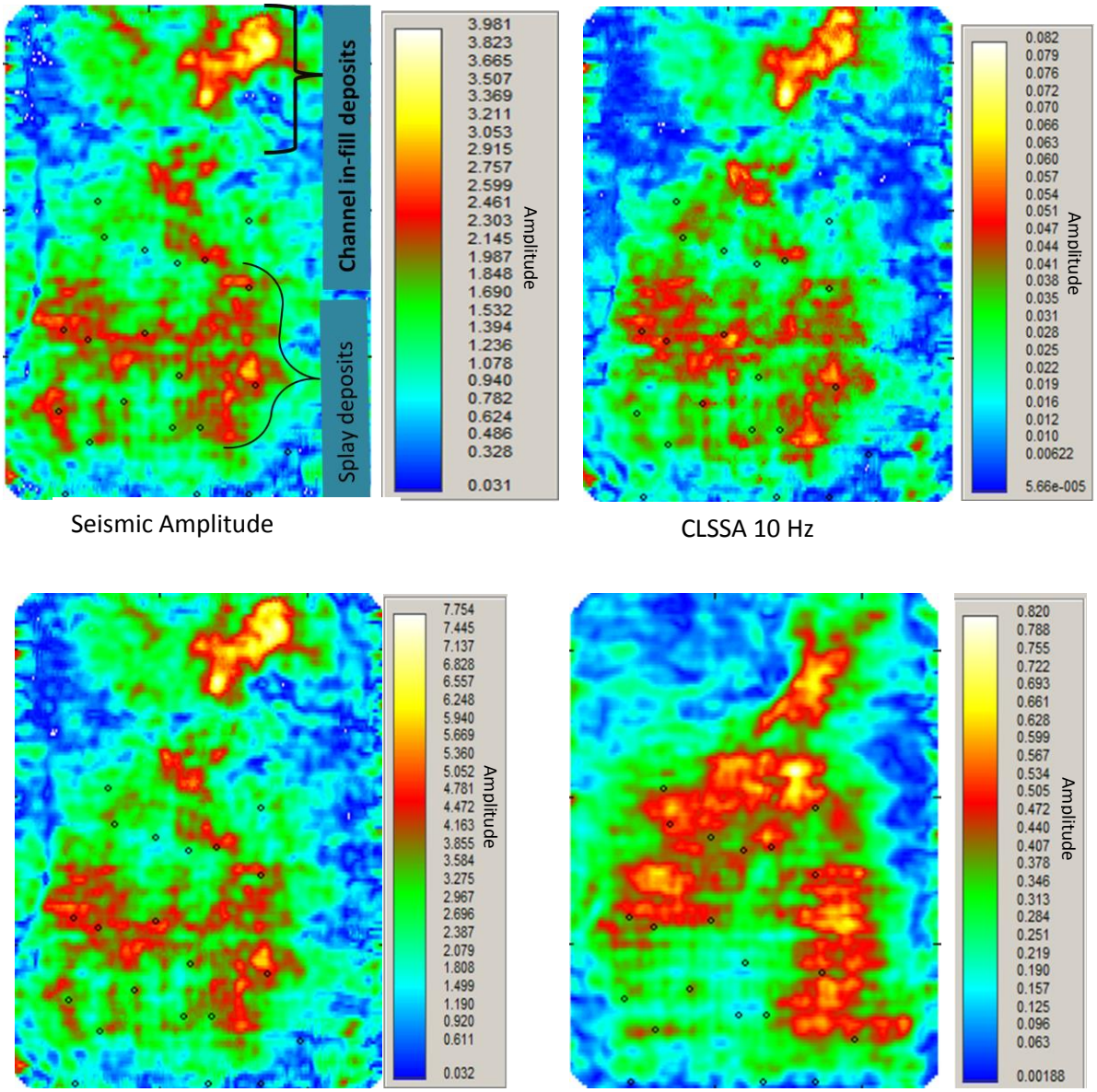

Seismic Amplitude

CLSSA 10 Hz

DFT 10 Hz

CWT 10 Hz

Figure 16. Comparison between seismic amplitude map and CLSSA, DFT and CWT spectral maps at peak frequency (20 ms analysis window). CWT is not dependent on window, so it is the same for 20 ms and 40 ms window. (a) Seismic amplitude map (b) CLSSA 10 Hz (c) DFT 10 Hz (d) CWT 10 Hz.

CHAPTER FOUR

PRINCIPAL COMPONENT ANALYSIS

Multidimensional variables are difficult to visualize in a meaningful manner. Reducing the dimensionality into clusters or indices eliminates unwanted variables, while preserving the most fundamental data values. In this chapter, I will discuss Principal component Analysis: theory and interpretation as it applies to the spectral attributes, then conclude the chapter by discussing about spectral blending of frequencies.

Principal component analysis is a type of factor analysis that uses linear mathematical concepts of eigenvalue and eigenvectors to rotate a data to a new coordinate system, such that the new correlation of the new set of values is different from the initial values. Principal Component Analysis or PCA for short is a statistical procedure used in multivariate analysis that uses an orthogonal transformation to convert a set of correlated variables or data points into linear uncorrelated values called principal components. This technique is a dimensionality reduction tool that truncates the number of dimensions to be retained within a data set. Eigenvalues usually decides the number of variables to be retained with the greatest variance in the data lying on an orthogonal direction called principal components. The transformation occurs in such a manner that the first PC or principal component has the largest variance in the data with the condition that it is orthogonal to later components.

In a set of real data variables making up a symmetric square matrix, the product of the data variables and the eigenvector from the matrix gives a scalar product multiplied by the eigenvector. The relationship below illustrates this point. The scalar quantity signifies the highest variance in the data, hence earned the name eigenvalue.

$$\bar{\bar{Q}}\,\bar{\bar{V}} = \lambda\,\bar{\bar{V}}$$

$\bar{\bar{Q}}$ is a real and symmetric square matrix having the eigenvector $\bar{\bar{V}}$ (a non-zero square vector matrix). λ is the eigenvalue, which when scaled with the eigenvector gives back the matrix of $\bar{\bar{Q}}$. This illustrates that the relationship between eigenvalue and eigenvector is that of a scalar multiplier, where the scalar multiplier represents the highest variance in the original square matrix. To further put this in the context of PCA, the eigenvector corresponding to the largest eigenvalue gives the first PC, and the second largest variance gives the second PC, and so on, with the condition that all the PC's must be orthogonal to each other. Figure 17a illustrates in a simplistic manner how the PC's are generated. From the figure, two variables X and Y of different dimensions are related on a plot. The orientation of the points establishing the relation between them is ellipsoidal in shape, such that two vectors passing through the points can be used to determine the plane of best correlation between the two variables. The data space of the points could be said to be representative of smaller dimensions of the larger sets, duly represented by x' and y' vectors respectively. The longer vector line has better line of fit to the points than the shorter vector line. A point to note is that the two vectors are orthogonal to each. However when the two axes are rotated as shown in fig17b below, we have a new set of correlation and orientation of the data points. The

new axes now form the PC's. From the figure, two points lie on the PC2 while four points lie on PC1.

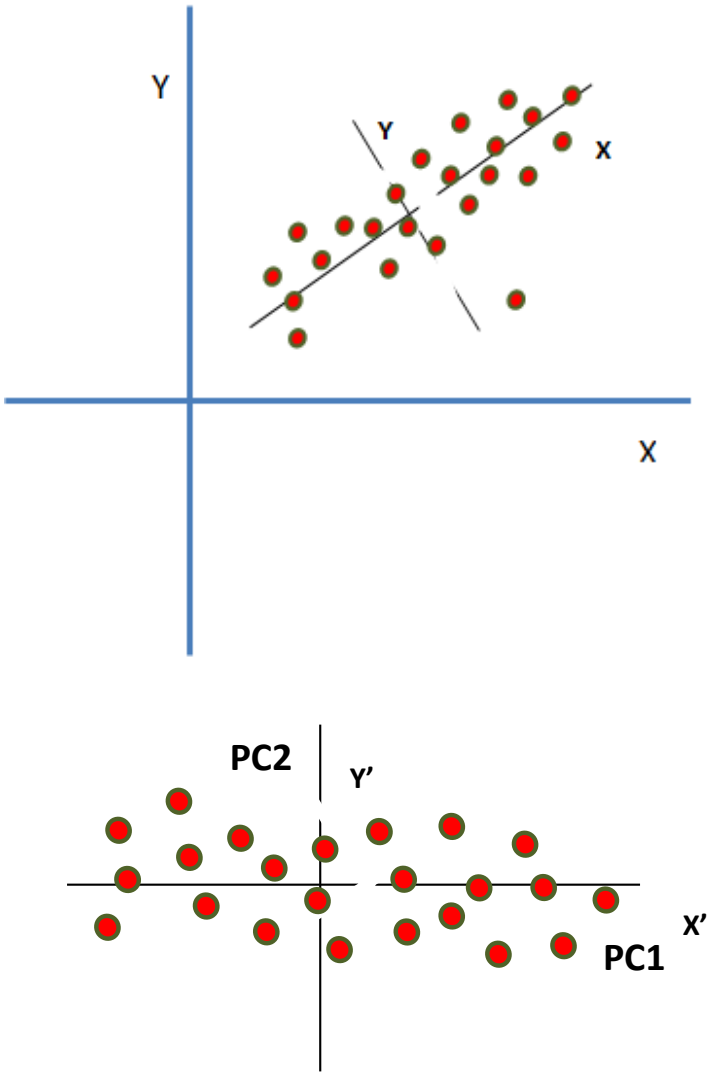

Figure 17 Illustration of the concept dimensionality reduction and axes rotation in principal component analysis (modified after, Holland.M.S.(2008)

There are basically two types of matrix systems used in PCA computation: covariance matrix and correlation matrix. Covariance matrix measures the dimensionality relationship between two or three variables with respect to each other (their mean value). Usually this type of matrix is used when the data variables are in different units. Correlation matrix on the other hand, standardizes the variables to zero mean and unit standard deviations. This type of matrix is generated using a square matrix containing the correlation coefficients between every pair of the values. The calculated mean is subtracted from each value to generate the covariance and variance between each pair of the values. Final correlation matrix is attained after the values are normalized by the covariance with the square root of the values, or standard deviation of the values. Data points that do not correlate well with other data points are not preserved, hence reduces the size of the data.

Principal components are independent only when the data is said to be normally distributed. PCA is sensitive to the scaling of the original variables depending on the purpose of the applications. The reliability of this method has found applications across various disciplines from pattern recognition in the area of geophysics to image compression, meteorology, agriculture, remote sensing, to mention but a few.

Historically speaking, PCA as it is used today in statistics was first introduced by Pearson (1901) and Hotelling (1933). Though earlier inception of this method in data analysis can be traced back to the 19^{th} century to Beltrami (1873) and Jordan (1874), where they worked independently using Singular Value Decomposition (SVD) in a

manner akin to PCA. Pearson (1901) used geometrical optimization problems to determine the best point, lines and planes can fit in a dimensional space. Hotelling however was spurred to work on PCA when he noticed outlier points existing independently from a cluster of data points. He tagged them ''fundamental independent variables''. The variables he noted, contributed to the overall variance in the data which he later christened Principal components. He used the Lagrange multipliers in his computation and ended up with an eigenvalue/eigenvector problem. His methods differ from the typical Lagrange multiplier solution in that he used a correlative matrix than a covariance matrix, and the matrix notation is expressed as components in a linear functions manner (Joliffe, 2001)

4.1 Intrinsic Components of the Seismic Data

In Statistics, using a subset of a sample is advantageous as we have something more convenient to work with, while retaining the most intrinsic properties of the main data (Figure 17). The seismic data can be described in terms of continuity, redundancy and noise. Continuity here refers to the lateral nature of the geology that is expressed as interpolated seismic traces representing subsurface amplitude reflections. Qualitative structural and stratigraphic interpretation is achieved here after seismic processing. Redundancy is created by the spreading of seismic information from the reflectors in vertical and lateral directions as the waveform propagates. Majority are recorded as part of the data while some may be lost due to other seismic effects. Lateral redundancy is caused by the survey geometry and binning sizes, while the vertical redundancy is under the influence of bandwidth of the source wavelet that is less than the Nyquist

frequency for a seismic data with a sampling rate of standard 4 ms. Correlation is strongest between traces as the true dimensionality of the data is simpler than the number of traces in the samples. Noise such as ground rolls and surface air waves are integral part of the seismic data, creating a tradeoff between resolution and noise suppression during the processing. (Coleou et al., 2003)

4.2 Method

To compute the principal component representative of the variability in the data, the program (matlab code) adopts a method similar to Brito's (2010), where a PCA window operator is defined (Figure 18) corresponding to a small analysis window. Unlike her approach, the program creates a matrix system from the inlines and crosslines spanned by the window operator. Note that the black circle in the figure represents the PC sample in the PC operator .In this computation, the window spans 3 Inlines and 3 crosslines at each point. It then moves across the entire time window length of interest at that moment. When I used smaller windows such as 100 ms, the program generates a 3×3 matrix using the inlines, crosslines and the size of the window to generate the total number of samples to be used in the computation. With a 100 ms window for example, we have 3×3×100=900 samples. This procedure works through the 15 frequency volumes for the separate spectral decomposition volumes for both CLSSA and DFT as the input attribute variables. The attribute volumes used are from 10-80 Hz, at 5 Hz interval. A starting frequency of 5 Hz was initiated but the program generates a complex number. This may be indicative of the sensitivity of the program to input variables that have data only, as the 5 Hz could have less data points and be noisy. Inlines and

crosslines of the PC operator are taken in as an ordered set of vectors, taken from the entire seismic volume covering the analysis window to represent a statistical mass of samples for the correlation matrix. Amplitudes were first normalized in all the 15 frequency cubes for the different algorithms, as some volumes have higher amplitudes than others. Normalization of this type in qualitative studies is not detrimental. Cross correlation of the frequency volumes with itself and the number of samples from the analysis window, creates a correlation matrix coefficient. The next stage was to decompose the correlation coefficient into scalar eigengenvalue $\boldsymbol{\lambda}$ **,** and $\bar{\mathbf{v}}\mathbf{\times 1}$ eigenvector, using the relation above to generate the eigenvectors. The eigenvector with the highest eigenvalue becomes the 1st PC, the next in variance, which must be orthogonal to the first gives the second PC. The final output cube is not in segy, so the program reshaped it back into segy format. In this work, I interpreted only the first three PC's as they seem to contain valuable information.

The technique employed in this PCA is data driven and image features beyond the bandwidth of the spectral decomposition attributes. Integration of multiattributes analysis fortifies our confidence in understanding reservoir stratigraphy obscured by interference pattern. My approach here was to use the most-relevant-attributes volume that highlights an aspect of the feature and discard those that don't. The most meaningful attributes information was projected unto a series of new coordinates preserving the most distinctive outline of the feature. This transformation optimizes the stratigraphic feature, hence subduing redundancy in the data.

Principal component analysis utilizes all the data available. When the data points however are less than the number of input variables, then the use of a covariance matrix would be suitable to generate the PC's. On the other hand when the number of input variables are less than the data points, then there is need to standardize the input parameters using the relationship:

$$A=B^{T}.C$$

Where A is the number of data points, B transpose is the matrix of the principal components and C is the input variable matrix. Standardization subtracts the mean value from the each observation points and divides by the standard deviation. The division limits the deviation value to range from -1 to +1. PCA generated in this way is by correlation matrix.

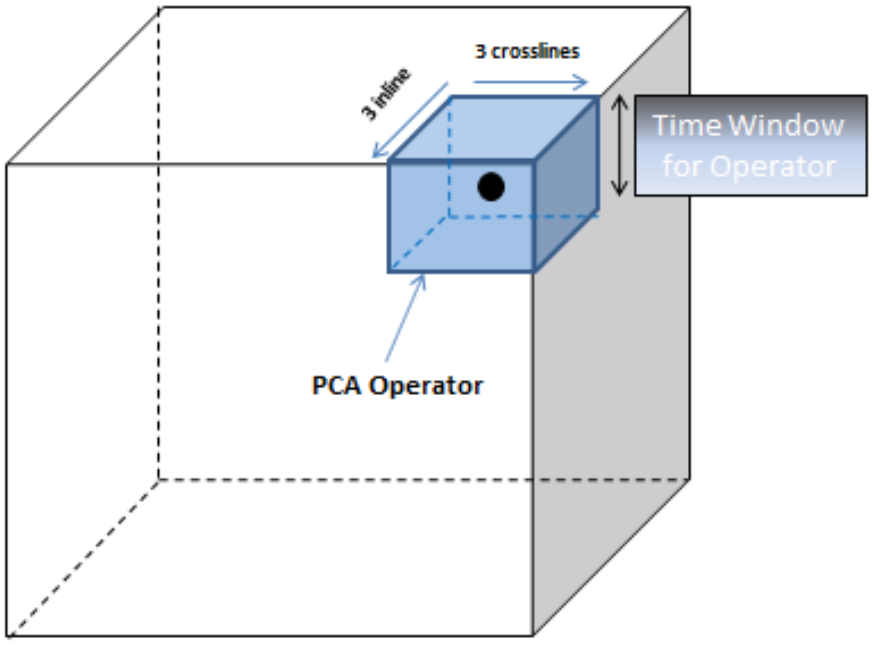

Figure 18. Schematic illustration of the PCA operator within the PCA window (Modified from Brito, 2010)

4.3 Interpretation

In this work I applied the spectral decomposition attributes directly to visualize subtle features, while I used the frequency volumes as input variables in the PCA computation. I utilize the frequency volumes that were generated at 20 ms and 40 ms analysis window respectively, but the results for the 40 ms were very noisy as the PC has nothing tangible in them. I concentrated on the 20 ms analysis window as it enhanced my interpretation. On the PCA window size, I tried 20 ms and 40 ms window during computation but I got nothing but noise. I tried smaller windows at 100 ms and 52 ms, which gave me something to look at. The program couldn't generate the PC's at 50 ms window, because it can only sample the volumes at multiples of 4 ms interval, which makes 52 ms closer to 50 ms. Results for CLSSA and DFT at 52 ms will be attached in the appendix section of this work.

Figure 19 b-d shows the PCA at 100 ms for CLSSA at 20 ms analysis window. PC1 did not highlight the splay deposits as they fall below tuning. The only prominent feature on this PC is the channel in fill sandstone. AS the number of PC's increases, the output gets noisier. A possible explanation for this is that the PC's are uncorrelated after the axes rotation. Another reason could be that the amplitude normalization could be detrimental to the CLSSA to have suppressed all the valuable amplitude of significance. As shown in the figure, CLSSA does poorly than the seismic in the PC domain. On the other hand, PC1 for DFT at 20 ms analysis window shows a better feature than the

seismic (Figure 20b-d). Even PC2 does somewhat better than the seismic. Figure 21 b-d shows a comparison between the seismic, PC1 DFT, spectral maps for CLSSA at 40 ms window, and DFT at 20 ms window respectively. I used these windows because they are the best spectral frequencies that show the features better. From the figure, PC1 DFT shows an enhanced channel in-fill deposits, and the splay deposits geometry appears more delineated compared to the spectral maps of CLSSA 10 Hz at 40 ms analysis window, and DFT 10 Hz at 20 ms window. Figure 22 a and b, show plots of the five PC's eigenvectors for CLSSA and DFT. In figure 22 a, the variation of the spectral energy are more concentrated on the high frequency end than the low frequency. This could indicate that there is more concentration of the high frequency features in the PC's than the features are at low frequency. For the DFT, the spectral energy is somehow evenly distributed on the low and high frequency end for the entire PC band. A likely reason for better correlation of the DFT PC's over CLSSA could be that the PC1 spectrum is more relaxed and undulating creating a smoother match of variables than the CLSSA that has a taut curve.

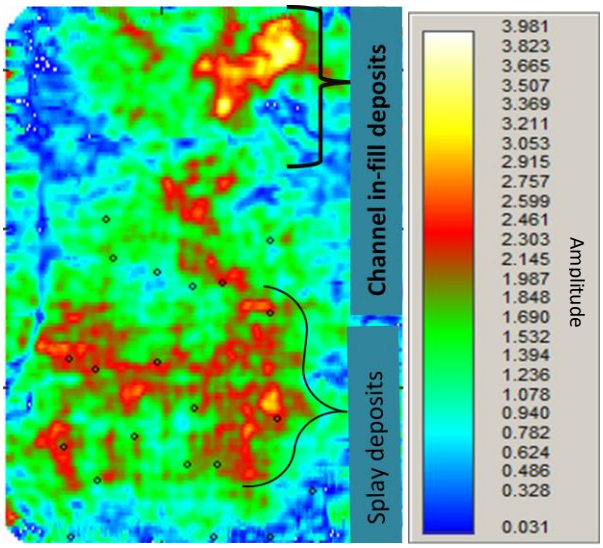

(a) Seismic Amplitude

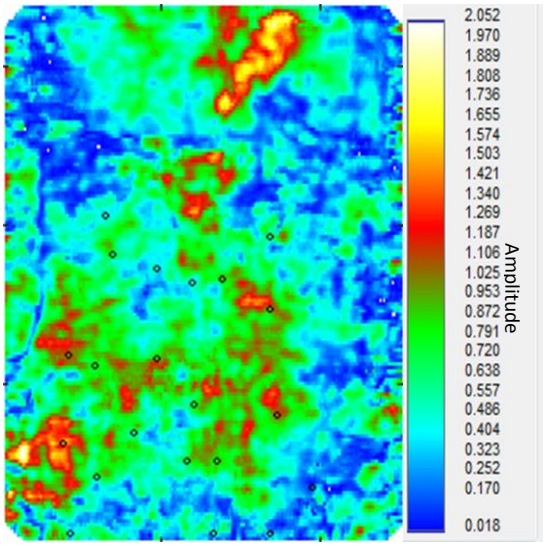

(b) CLSSA PC1

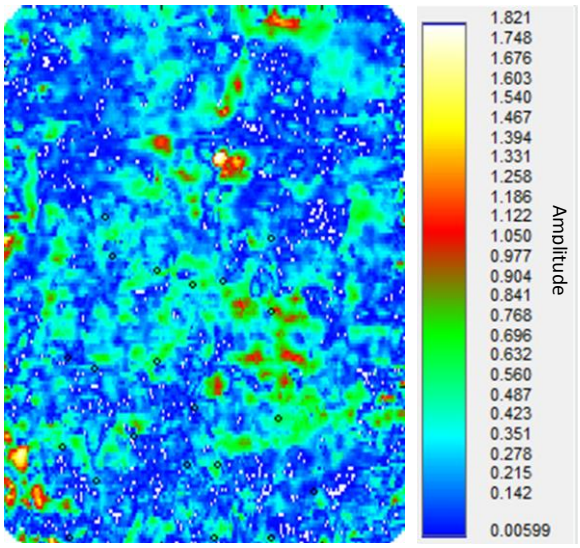

(c) CLSSA PC2

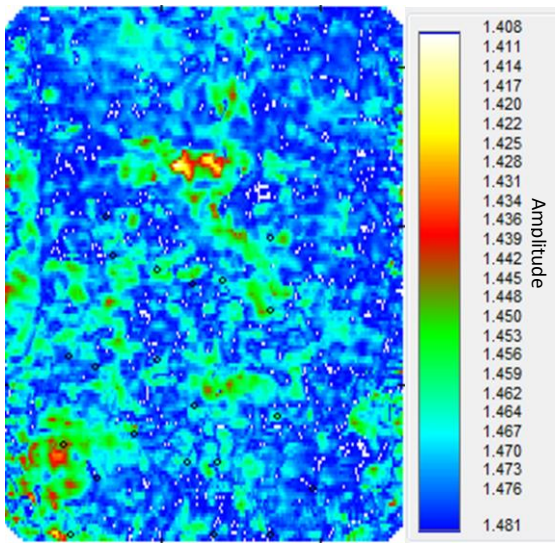

(d) CLSSA PC3

Figure 19. Comparison between seismic amplitude and the PC's for CLSSA. PC analysis window is 100 ms. (a) Amplitude map (b) CLSSA 1st PC (c) CLSSA 2nd PC (d) CLSSA 3rd PC. CLSSA PC's get noisier after axis rotation of the input attributes, leading to obliteration of the feature as PC value increases.

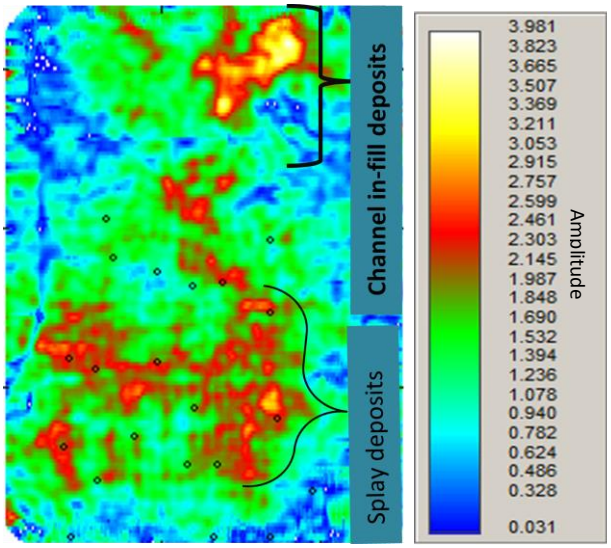

(a) Seismic Amplitude

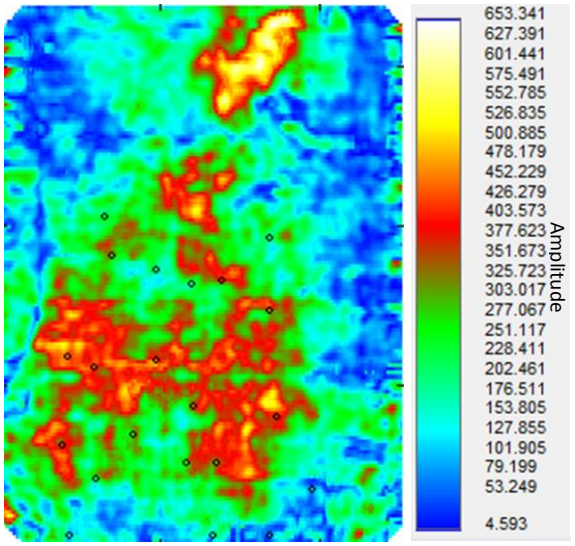

(b) DFT PC1

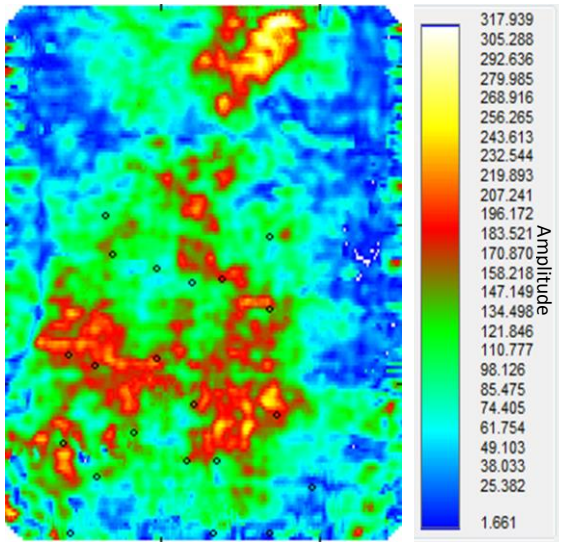

(c) DFT PC2

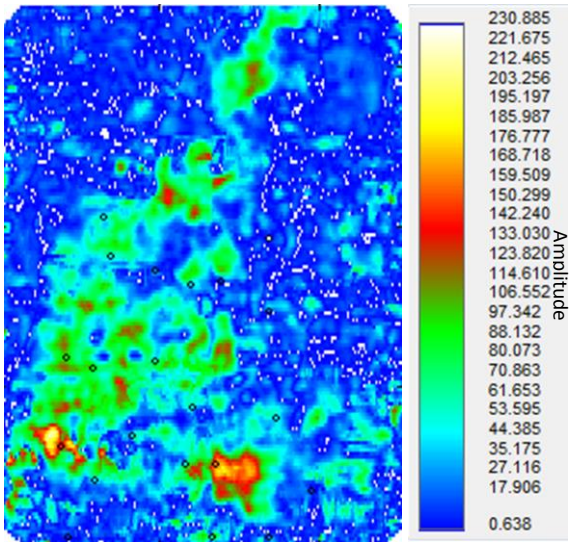

(d) DFT PC3

Figure 20. Comparison between seismic amplitude and PC's for DFT. The PCA analysis window is 100 ms. (a) Seismic amplitude map (b) DFT 1st PC (c) DFT 2nd PC (c) DFT 3rd PC. There is a strong correlation of the DFT attributes after axis rotation, leading to superior delineation of the 'D' Sand series reservoir.

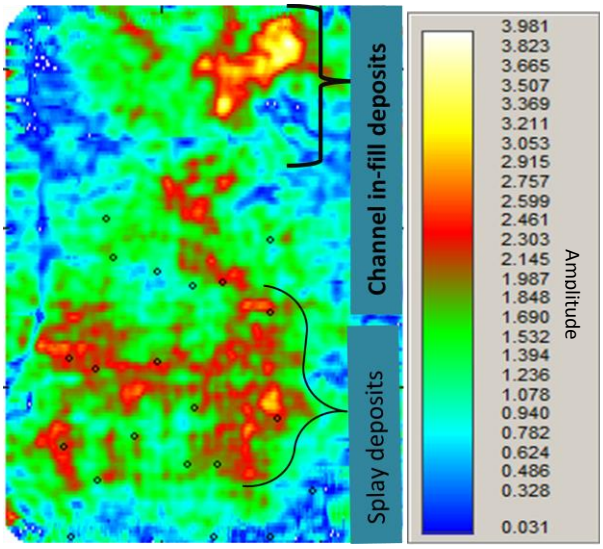

(a) Seismic Amplitude

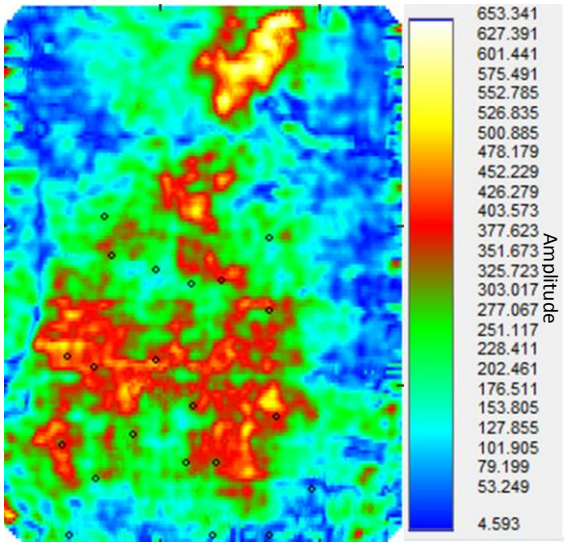

(b) DFT PC1 at 100ms

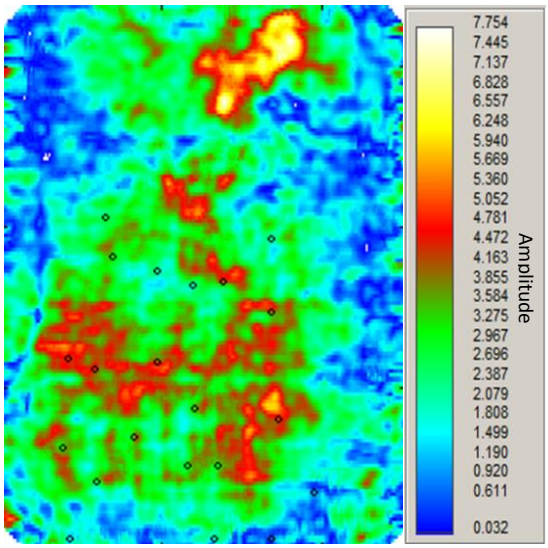

(d) DFT 10 Hz

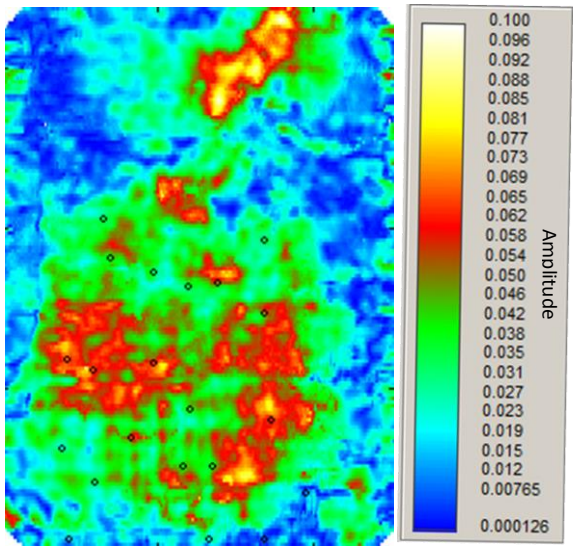

(c) CLSSA 10 Hz

Figure 21 Comparison between DFT PC1 at 100 ms widow and spectral maps at 10 Hz dominant frequency for CLSSA at 40 ms window, and DFT at 20 ms window. (a) Seismic amplitude (b) DFT 1st PC (c) DFT 10 Hz (d) CLSSA 10 Hz. DFT 1st PC goes beyond the bandwidth limit of the spectral attributes..

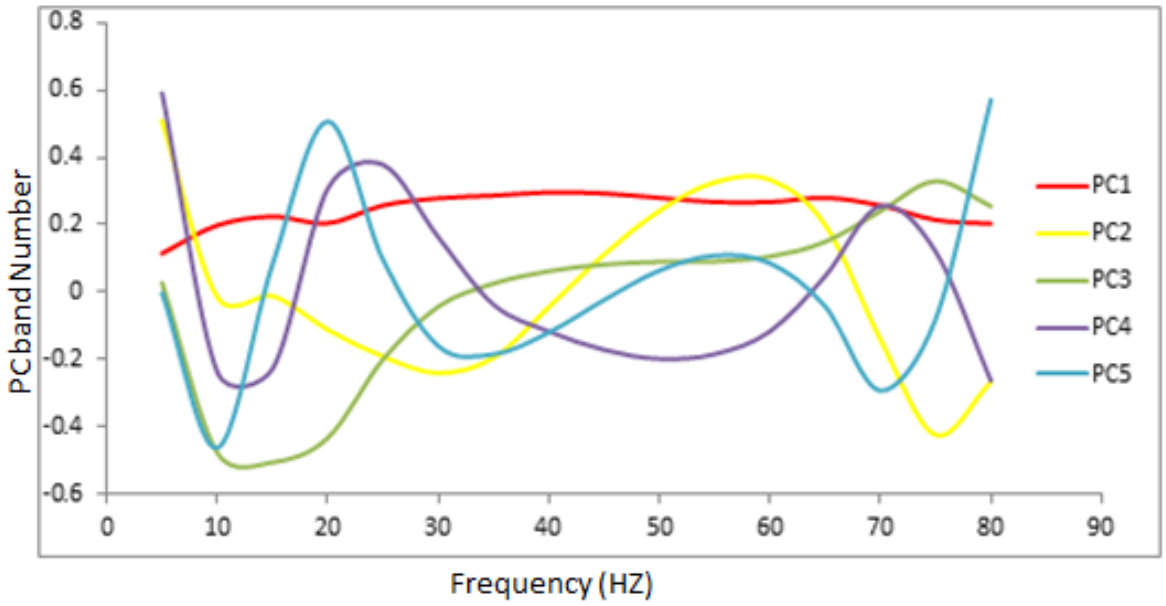

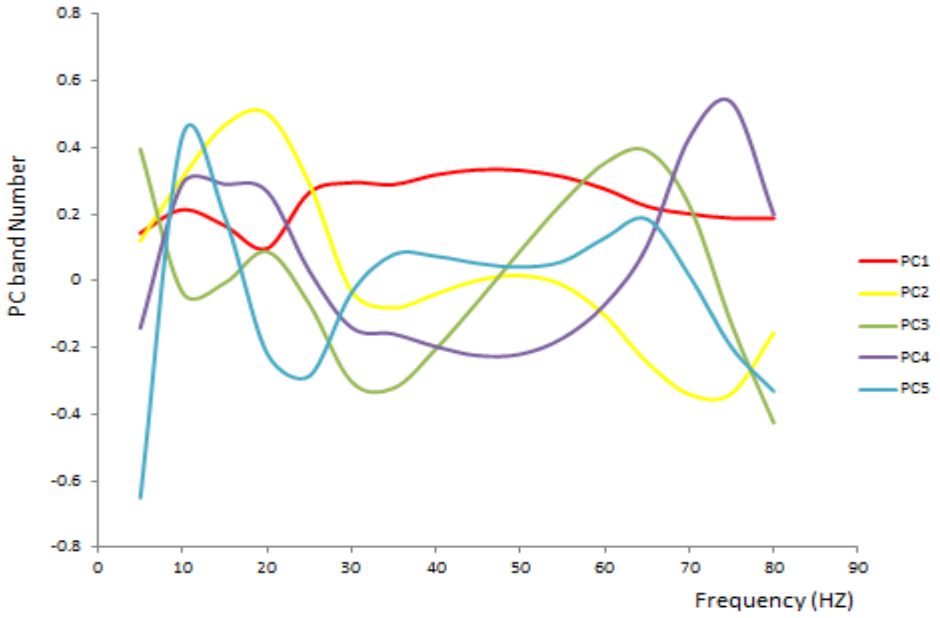

Figure 22 First five principal spectral components computed from the eigenvectors for (a) CLSSA 100 ms PC window (b) DFT 100 ms PC window

4.4 Color Blending (RGB) display.

The amount of information that a time slice or horizon conveys to an interpreter is enormous. The level of details depends on how he can intuitively separate the features of interest from that which is not. Colors were first introduced by Taner and Sheriff (1977), and Lindseth (1979) to convey information in a logical way during interpretation. Different color schemes have been used over time. HLS (Hue, Light, Saturation), CMYK (Cyan, Magenta, Yellow, Black), Red, Green, Blue (RGB) etc. The color schemes show gradation and contrast on a horizon in a lateral manner, which has a link to thickness and reflection coefficient. Colors are an essential part of interpretation as a reflection from a given lithology is easily discerned from the background reflection, e.g. sand that is gas charged will exhibit a different color from a sand body that is not. Similarly, high amplitude channel sand will show up differently from low amplitude channel sand. Gradation in color added to amplitude will help to locate channels, streams and depositional environment in a wide range of densities (Brown, 2011).

RGB is a powerful tool that appends the amplitude of frequency into a single map display. Frequency blending exhibits the potential to enhance subtle lithological changes using the dominant color bands sensitive to thickness and acoustic impedance variation. Multiattributes RGB display assigns a color to each frequency volume. RGB works very well where the input variables are highly correlated and the final blend will append the three primary colors into a composite display that contain mixtures or specs

of red, green or blue colors relative to the sensitivity of the features to the color band. This color blending can be said to be a noise suppressor as systematic variation in the different volumes are only represented in the color trends on display.

Subtle stratigraphic features limited from seismic resolution by interference patterns can reveal startling features when different colors are combined. RGB bands are sensitive to bed thickness and acoustic contrast of geologic features, and are strongly correlated to the tuning frequency of the features. Color blending is used here to show the geometry and extent of the stratigraphic feature by blending different frequency volumes.

RGB depends upon the dominance of the individual color assigned to a frequency value. Combination of the three colors in equal proportions yields white light. The dominance of one over the other however, will exhibit that color on the feature. When two colors dominate, the color on display will be an admixture of the two colors.

There exist an inverse relationship between frequency and the thickness of a bed. Low frequencies highlight thick portions of a layer while high frequencies highlights thin layers depending on the tuning frequencies. Here, I blended 10-15-20 Hz frequency volumes of the CLSSA at 40 ms window into a single map. I made that decision because the preceding result shows that it has the best display of the features. Figure 23 shows the RGB display compared with the original seismic. The stratigraphic feature appears magenta because the dominant colors that highlight the features were red and blue, meaning that the 10 Hz and 15 Hz frequencies contributed in equal amount. Similarly the background appears green with specs of black. Notice how the feature is more

extensive than the broadband amplitude. Figure 24 shows the spatial extent of the true geometry without interference effects. From the figure and all the preceding analysis, we can deduce the geological history of the thin layer here to be of a channel axis that is filled to the brim with sandstone deposits. The deposits overflew its banks to form splay away from the in-fill.

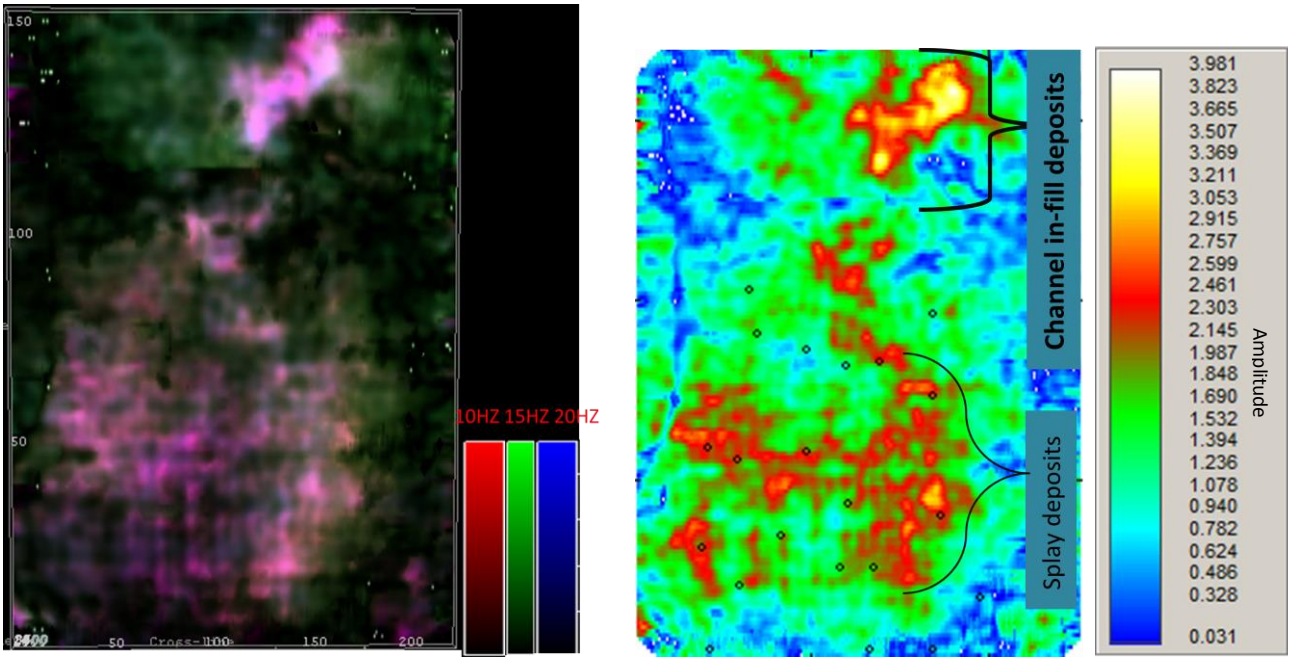

(a) RGB composite display of 10 Hz-15 Hz-20 Hz

(b) Seismic Amplitude

Figure 23. Comparison between (a) Red-Green-Blue (RGB) display using the best tuning frequencies of 10-15-20 Hz and the (b) Seismic amplitude. Notice the spatial extent of the feature from the frequency blend. The magenta color result from the dominance of the red and blue colors i.e. 10 Hz and 20 Hz, while the green color assigned to 15 Hz highlights the outer layer of the stratigraphic feature

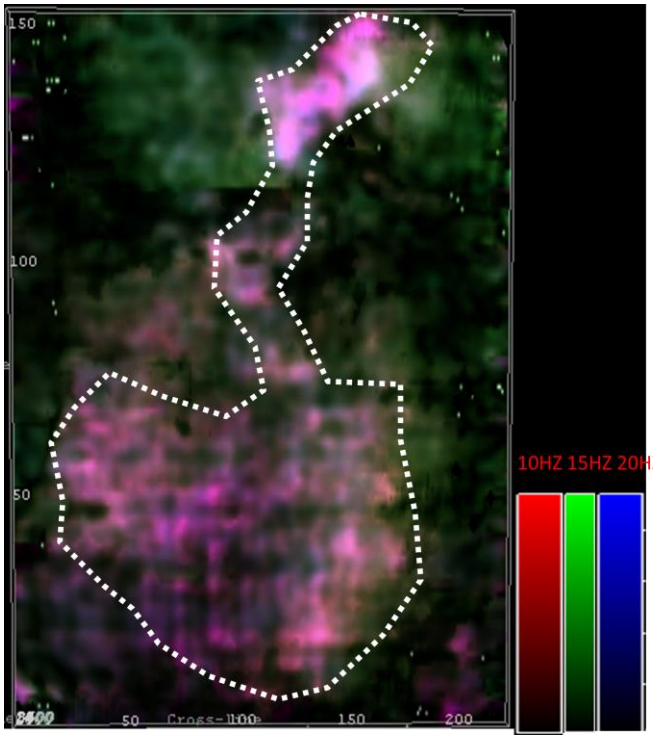

Figure 24 RGB display showing the spatial extent of the stratigraphic feature using the best tuning frequencies of 10-15-20 Hz. The magenta color corresponding to the feature shows the dominance of the 10 Hz and 20 Hz frequencies.

CHAPTER FIVE

SUMMARY AND CONCLUSIONS

This work has shown that we can image subtle features beyond the bandwidth limit resolvable by the spectral decomposition attribute method, when the coordinates of the frequency attributes are rotated in a manner that creates a synergy between spectral decomposition and principal component analysis. A 'D' sand series of the middle Frio Formation Stratton field, was further enhanced to show channel in-fill deposits that was deposited laterally with splay sand bodies. The stratigraphic geometry on the seismic amplitude map was enhanced by spectral attributes but a better enhancement was obtained using principal component analysis.

The advantages of using a windowed data within a spectrum translate to a better Heisenberg uncertainty product, where the spectral resolution is superior over using the spectrum of the windowed data. This is observable for both the long and short windows of spectral decomposition. Discrete frequencies reveal that CWT has poor frequency resolution due to amplitude smearing at low frequencies and cannot resolve high frequency events. DFT at short windows resolves the events in the same magnitude like the seismic amplitude at low frequencies. As the window size doubles, the bed thickness is better resolved at higher frequencies, and poorly at lower frequencies. This is an indication that the Heisenberg uncertainty product is inconsistent for the DFT. CLSSA on the other hand resolves the features at low frequencies beyond the seismic

resolution. Shorter windows see CLSSA losing the peak frequencies as less of the feature is captured. Therefore in this basin, CWT is not a recommended method to administer, though it may work greatly in other basins. DFT using running windows shows a lot of inconsistencies with fluctuating Heisenberg Uncertainty product as the peak frequencies differ. CLSSA at larger windows highlights the subtle features better as the tuning frequencies tends to be more sensitive at this window length. Smaller windows might be appropriate for spectral inversion purposes as the spectrum of the data is very taut.

Preserving the direction of maximum variance at smaller windows goes beyond the spectral decomposition limit to enhance subtle features that are absent on the spectral maps. DFT produce higher fidelity than the CLSSA at 40ms windows. A possible reason might be that the attributes volumes may be well correlated during the axis rotation. Another likely reason might be Heisenberg Uncertainty product, though better in the CLSSA at different windows, it may be distorted after axis rotation. Surprisingly, at lager windows DFT loses the correlation of the attributes as the PC's perform poorly compared to CLSSA. Smaller PC windows forfeit the spectral resolution for both DFT and CLSSA, even though CLSSA show aspects of the feature better. At larger windows, PC's of CLSSA are uncorrelated as the DFT performs better than the best CLSSA spectral map peak frequency.

Larger spectral decomposition windows delineate the stratigraphy better than shorter windows. Interleaving the frequency volumes at lower frequencies by assigning a component of the primary color spectrum , shows the entire outline of the features, assuming that the acoustic contrast are relatively uniform and the tuning frequencies of

the bed resonate at a single frequency. The geological history I could deduce from the above analysis is that, there was deposition of siliclastics sediments into the channel axis. The axis was filled to its brim and then overflew to form splay deposits far away from the channel axis. Finally, a point to note here is that the results obtained here is restricted to this field. Using this method in another basin may produce different results.

REFERENCES

Bebout, D.G., RG. Loucks, and A.R. Gregory, 1977, Test site for geothermal well-Frio Sandstone. Texas Gulf coast; AAPG Bulletin v.61, p.765-765.

Brito, Maria, 2010, Principal Component Analysis for Stratigraphic imaging and facies prediction the Gulf of Mexico, M.S. Thesis

Brown. A.,R., 2011, Interpretation of Three Dimensional Seismic Data, 7th Edition, AAPG Memoir 42, SEG Investigation No. 9.

Castagna, J. P., S. Sun, and R. W. Siegfried, 2003, Instantaneous spectral analysis: Detection of low-frequency shadows associated with hydrocarbons: The Leading Edge, **22**, 120–127.

Castagna,J.P.,2004, Spectral Decomposition and High Resolution reflectivity inversion, presentation at Oklahoma city SEG section meeting.

Chakraborty, A. and Okaya, D., 1995, Frequency-time decomposition of seismic data using wavelet-based methods: Geophysics, Soc. of Expl. Geophys., 60, 1906-1916.

Chopra, Satinder, John P. Castagna, O. Portniaguine, 2006, Seismic resolution and thin-bed reflectivity inversion: CSEG Recorder, v.
31, no. 1, p. 19-25.

Coleou T, Poupon. M & Azbel K. 2003. Interpreter's Corner - Unsupervised seismic facies classification. A review and comparison of techniques and implementation. The Leading Edge, 22: 942-953.

Gabor, D., 1946, Theory of Communication, IEEE.V93 P.429-441

Galloway, W. E., 1977, Catahoula Formation of the Texas Coastal Plain-depositional systems, composition, structural development, groundwater flow history, and uranium distribution: The University of Texas at Austin, Bureau of Economic Geology Report of Investigations No. 87.- 1982, Depositional architecture of Cenozoic Gulf Coastal Plain fluvial systems, in Ethridge, F. G., and Flores, R. M., Eds., Recent and ancient nonmarine depositional environments: Models for exploration: SEPM Spec. Publ. No. 31, 127-155.

Galloway, W. E., Hobday, D. K., and Magara, K., 1982, Frio Formation of the Texas Gulf Coast basin-depositiona1 systems, structural framework, and hydrocarbon origin, migration, distribution, and exploration potential: The University of Texas at Austin, Bureau of Economic Geology Report of Investigations No. 122.

Guo, H, Lewis. S and Marfurt.K.J. 2008, Tutorial: Mapping multiple attributes to three- and four-component models, GEOPHYSICS VOL 73,No.3 P.W7-W19.

Guo. H., Marfurt.K.J. And Liu. J., 2009, Principal Component Spectral Analysis, GEOPHYSICS, VOL 74, NO 4, P.P35-P43.

Hardage, B.A., Lcvey, RA., Pendelton, V., Simmons, J., Edson, R., 1994, A 3-D seismic case history evaluating Fluvially deposited thin-bed reservoirs in a gas-producing property: Geophysics, 59, 1650-1665.

Hall, M,. 2006, Resolution and Uncertainty in spectral decomposition, First Break volume 24, p 43-47.

Holland.M.S. 2008, Principal Component Analysis, p 1-10.

James.J.F, 2011, A student's Guide to Fourier Transforms with Applications in Physics and Engineering.

Jirik, L.A., 1990, Reservoir heterogeneity in middle Frio fluvial sandstones: case studies in Seeligson field, Jim Wells County, Texas: Gulf Coast Association of Geological Societies Transactions, v. 40, p. 335-35 1.

Jollife.I.T, 2001, Principal Component Analysis, p. 6-9.

Kerr, D.R., and Jirik, L.A., 1990, Fluvial architecture and reservoir compartmentalization in the Oligocene Middle Frio Formation, South Texas: Gulf Coast Association of Geological Societies Transactions, v. 40 p. 373-380.

Kosters, EC., Bebout, D.G., Seni, S.J., Garrett, C.M., Jr., Brown, L.F., Jr., and Tyler, Noel, 1989, Atlas of major Texas gas reservoirs: The University of Texas at Austin, Bureau of Economic Geology, p. 161.

Lindseth, R. O., 1979, Synthetic sonic logs — a process for stratigraphic interpretation: Geophysics, v. 44, p. 3–26.

Liner.C. 2010, An overview of wavelet Transform concepts and applications p.1-17.

McArdle.N.J and Ackers.M.A. 2012, Understanding seismic thin bed responses using frequency decomposition and RBG blending, first break volume 30, p. 57-65

Partyka, G., J. Gridley, and J. Lopez, 1999, Interpretational applications of spectral Decomposition in reservoir characterization: The Leading Edge, 18, 353–360.

Peyton, L., Bottjer, R., and Partyka, G., 1998,Interpretation of incised valleys using new-3D seismic techniques: A case history using Spectral Decomposition and coherency, The Leading Edge, **17**,No. 9, 1294-1298.

Polikar,R, 1996, Wavelets, users.rowan.edu/~polikar/WAVELETS/WTpart2.html

Portniaguine, O., and M. S. Zhdanov, 1999, focusing geophysical inversion images: Geophysics, 64, 874–887.

Puryear.C.I., Tai.S., Castagna. J.P., 2008, Comparison of frequency attributes from CWTand MPD spectral decompositions of a turbidite channel model. P. 393-397 SEG Las Vegas.

Puryear.C.I. Portniaguine.O.N., Cobos.C.M. And Castagna.J.P. 2012, Constrained Least Squares Spectral Analysis: Applications to seismic data. GEOPHYSICS vol 77, NO. 5, P.V143-V167.

Sinha, S., P. Routh, P. Anno, and J. P. Castagna, 2005, Spectral decomposition of seismic data with continuous-wavelet transform: Geophysics, 70, P19-P25

Taner, M. T., and R. E. Sheriff, 1977, Application of amplitude, frequency and other attributes to stratigraphic and hydrocarbon determination, *in* C. E. Payton, ed., and Seismic stratigraphy— applications to hydrocarbon exploration: AAPG Memoir 26, p. 301–327.

Tirado, S., 2004, Sand thickness estimation using spectral decomposition: M.S. thesis, University of Oklahoma.

Widess, M. B., 1973, How thin is a thin bed?: Geophysics, 38, 1176-1180.

APPENDIX

Comparison of PC's at 52 ms window for CLSSA AND DFT 20 ms analysis window

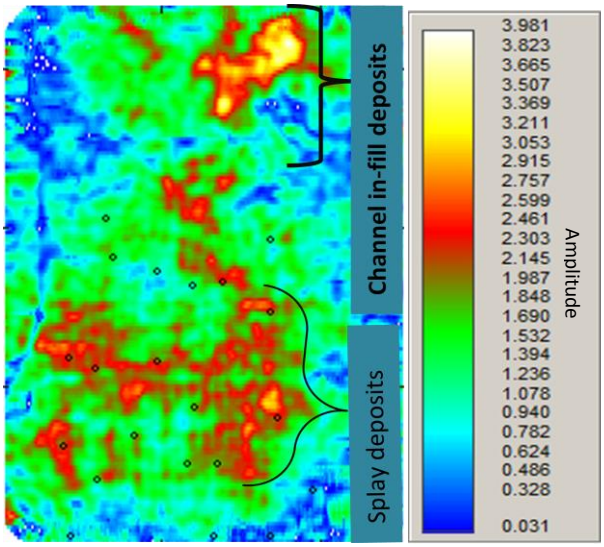

Seismic Amplitude

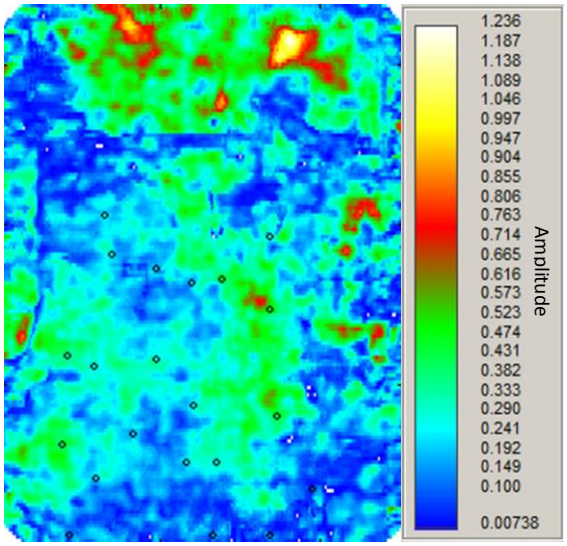

PC1 CLSSA

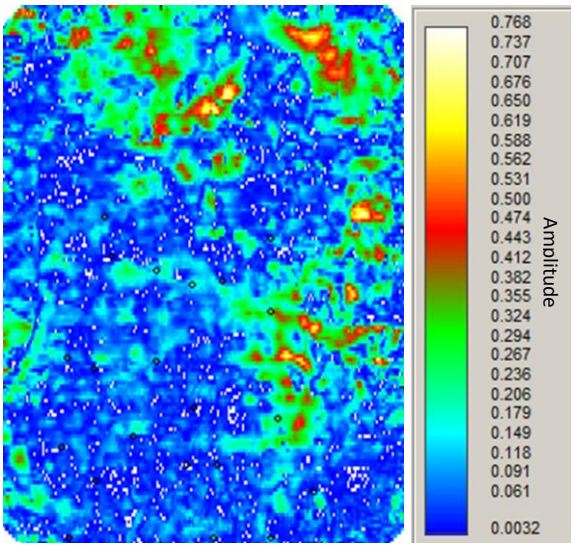

PC2 CLSSA

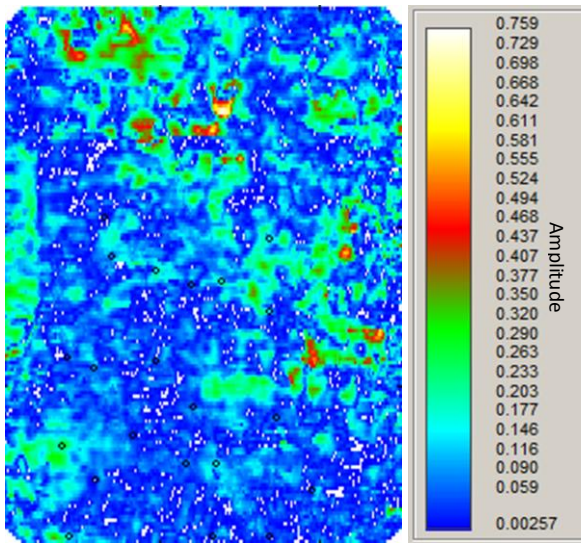

PC3 CLSSA

A1 Comparison between the seismic amplitude and PC's at smaller analysis windows. (a) Seismic amplitude (b) CLSSA 1ST PC (b) CLSSA 2ND PC (d) CLSSA 3RD PC. As the window size decreases CLSSA PC's become noisier and obliterated.

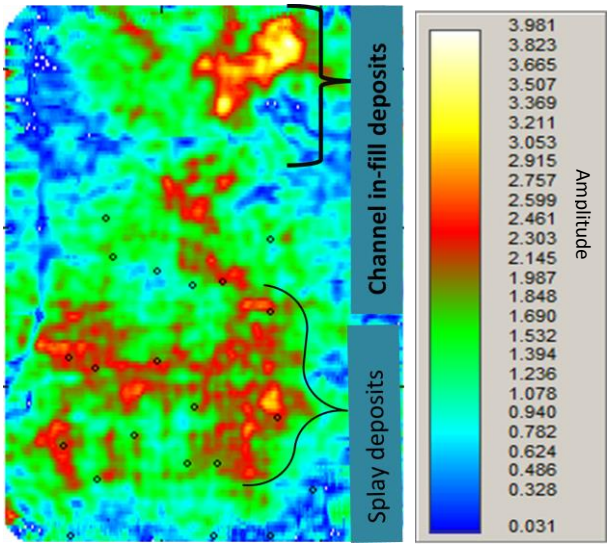

Seismic Amplitude

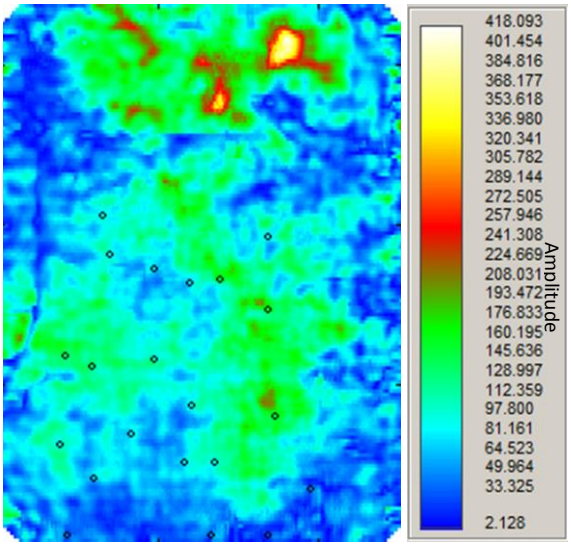

DFT PC1

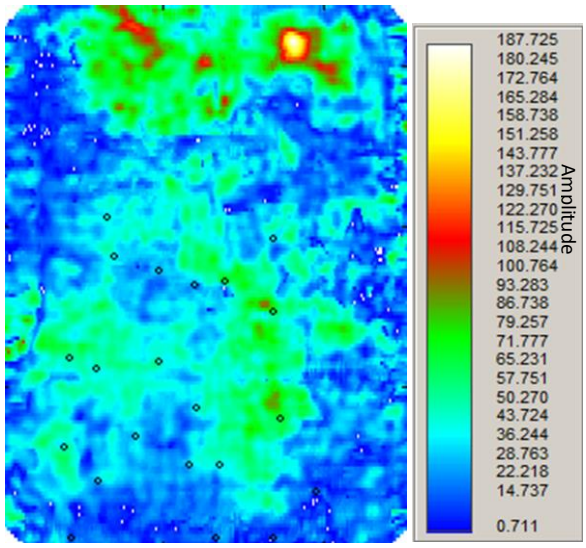

DFT PC2

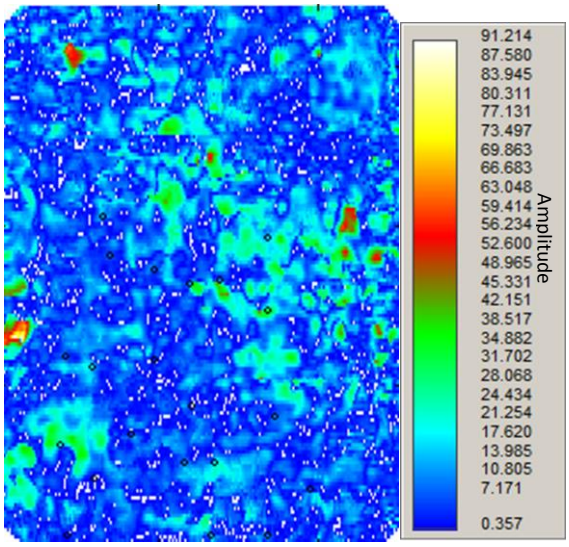

DFT PC3

A2 Comparison between the Seismic amplitude and PC'S at smaller analysis window (a) Seismic amplitude (b) DFT 1st PC (c) DFT 2nd PC (d) DFT 3rd PC. At smaller analysis windows, DFT PC'S become noisier.